

Study of Λ_c^+ , Σ_c , Ξ_c and Λ_b hypernuclei in the quark-meson coupling model

K. Tsushima¹ ^{*}, and F.C. Khanna^{2,3} [†]

¹Department of Physics and Astronomy, University of Georgia, Athens, Georgia 30602, USA

²Department of Physics, University of Alberta, Edmonton, Canada, T6G 2J1

³TRIUMF, 4004 Wesbrooke Mall, Vancouver, British Columbia, Canada, V6T 2A3

Abstract

Charmed and bottom hypernuclei with the low-lying heavy baryons, i.e., Λ_c^+ , Σ_c , Ξ_c and Λ_b hypernuclei, are studied systematically using the quark-meson coupling (QMC) model, which has been able to describe successfully the properties of nuclear matter, finite nuclei and strange hypernuclei. Effects of both the Pauli blocking originating from the underlying quark structure of baryons, and the $\Sigma_{c,b}N - \Lambda_{c,b}N$ channel coupling are taken into account at the hadronic level in the same ways as those included for the Λ , Σ and Ξ hypernuclei. It is shown that, although the total baryon density distributions and the scalar and vector potentials for these baryons are very similar to those for the hyperons with the same light quark numbers in the corresponding strange hypernuclei, the single-particle energies and the wave functions for them (e.g., for the $1s_{1/2}$ state), are very different. Our results suggest that the Σ_c^{++} and Ξ_c^+ hypernuclei are very unlikely to be formed, while the Λ_c^+ , Ξ_c^0 and Λ_b hypernuclei are quite likely. For the Σ_c^0 and Σ_c^+ hypernuclei, the formation probability is non-zero though small.

PACS: 24.85.+p, 14.20.Lq, 14.20.Mr, 21.80.+a, 21.65.+f

Keywords: Charmed and bottom hypernuclei, Single-particle energy levels, Heavy baryons in nuclear medium, Quark-meson coupling model

^{*}tsushima@physast.uga.edu

[†]khanna@Phys.UAlberta.CA

1 Introduction

Recently, we have initiated a systematic study for the properties of charmed and bottom hadrons in nuclear matter [1] based on the quark-meson coupling (QMC) model [2]. The results imply that the formations of B^- -meson nuclear (atomic) bound states, and charmed and bottom hypernuclei are quite likely. The formations of charmed and/or bottom hypernuclei, Λ_c^+ and/or Λ_b hypernuclei, were first predicted in mid-1970s by Tyapkin [3], and Dover and Kahana [4]. Later on theoretical studies [5, 6] as well as probability for experimental observation [7] were made. Further, we have studied the Λ_c^+ and Λ_b hypernuclei quantitatively [8] by solving equations of motion for a system of hypernuclei, embedding a Λ_c^+ or a Λ_b into the closed shell nuclear core, within the Hartree, mean-field, approximation using the QMC model. The results again support the possibility of existence of Λ_c^+ and Λ_b hypernuclei.

In this article we present the results studied systematically for charmed and bottom hypernuclei with the low-lying heavy baryons, i.e., Λ_c^+ , Σ_c , Ξ_c and Λ_b hypernuclei, using the QMC model. This is an extension of the studies made for the Λ , Σ and Ξ strange hypernuclei [9]. The extension is made in a straightforward manner, since the heavy baryons (as well as nucleon) are also classified by the quark constituents, and the QMC model can treat them on the same quark-based footing. One of the other important issues in this study is a consequence of the partial restoration of chiral symmetry in nuclear medium, for the low-lying heavy baryons containing charm or bottom quarks, and u and d light quarks. In such systems the light quarks are expected to play a vital role for the partial restoration of chiral symmetry in nuclear medium.

Concerning the experimental facility, the approved construction of the Japan Hadron Facility (JHF) with a beam energy of 50 GeV, will produce charmed hadrons profusely and bottom hadrons in lesser numbers, but still with an intensity which is comparable to the present hyperon production rates. Although the study of the presence of charmed and bottom hypernuclei may be in its infancy at present, it is clear that conditions for the experiments to search for such heavy baryon hypernuclei are now becoming realistic, and would be realized at JHF [10]. Thus, we think it is meaningful to consider such heavy baryon hypernuclei at this stage for the future experimental studies.

The QMC model (QMC-I), which is used in this study, has been successfully applied to many problems of nuclear physics, such as finite nuclei [11, 12], strange hypernuclei [9], nuclear matter [13], and many other problems including hadronic properties in nuclear medium [14, 15, 16, 17, 18, 19, 20]. (See also e.g., Refs. [21, 22] for earlier, different versions of QMC, and Ref. [23] for related work.) For example, the model was applied to the study of meson nuclear bound states [15, 16], J/Ψ dissociation in nuclear matter [18], D and \bar{D} productions in antiproton-nucleus collisions [19], and kaon properties in nuclear matter and kaon production in heavy ion collisions [20]. Furthermore, although only some limited studies for heavy mesons (not for heavy baryons) with charm in nuclear matter were made by the QCD sum rule (for J/Ψ [24, 25] and $D(\bar{D})$ [26]), a study for heavy baryons containing charm or bottom quarks was made only recently [1] using the QMC model. In particular, recent measurements of polarization transfer in the ${}^4\text{He}(\vec{e}, e' \vec{p}) {}^3\text{H}$ and ${}^{16}\text{O}(\vec{e}, e' \vec{p}) {}^{15}\text{N}$ reactions performed at MAMI and Jefferson Lab [27], support the medium modification of the proton electromagnetic form factors calculated by the QMC model, and the final analysis [28] seems to become more in favor of QMC [17], although still error bars may be too large to draw a definite conclusion.

There is also another version of the QMC model (QMC-II), where masses of the meson

fields are also subject to the medium modification in a self-consistent manner [29]. However, for a proper parameter set (set B) the typical results obtained in QMC-II are very similar to those of QMC-I. The difference is $\sim 16\%$ for the largest case, but typically $\sim 10\%$ or less. (For the effective masses of the hyperons, the differences between the two versions of QMC turn out to be less than $\sim 8\%$. See also Fig. 2 in Ref. [15] for the differences in the scalar potentials for the η and ω mesons in ^{208}Pb nucleus.) Since we use QMC-I, the differences in these numbers may be regarded as a measure of model ambiguities.

Certainly, the model has shortcomings that have to be improved eventually. Difficulties to handle the model will be increased rapidly in adopting the Hartree-Fock approximation even for nuclear matter [30], and further to include the Pauli blocking effect at the quark level. The effect of short-range quark-quark correlations associated with the nucleon overlap to treat high density nuclear matter was studied in Ref. [31]. With the addition of the correlations, the saturation curve for symmetric nuclear matter was greatly improved at high density. In addition, the $\Sigma N - \Lambda N$ channel coupling effect has not been implemented yet in a consistent manner with the underlying quark degrees of freedom [9]. (It should be mentioned that in the case of Σ hypernuclei no narrow states have been observed experimentally. It is unlikely that it will be possible to find such states in the present situation [32].) Furthermore, an application to double hypernuclei has not been attempted, although recently the existence was confirmed for small baryon number nuclei [33]. Nevertheless, there are some positive aspects of this model such as its simplicity and successful applicability, that we feel confident that the QMC model will provide us with a valuable glimpse into the properties of charmed and bottom hypernuclei.

In the QMC model, the interactions between nucleons are mediated by the exchange of scalar (σ) and vector (ω and ρ) meson fields self-consistently coupled to the quarks within those nucleons. One of the most attractive features of the QMC model is that it does not involve much in the way of additional complications to Quantum Hadrodynamics (QHD) [34]. Furthermore, it is systematically applicable to the studies of any hadron properties in nuclear medium [1, 14], as long as they contain at least one u or d light quark. Thus, we make use of the advantages of the QMC model, and study the low-lying charmed and bottom baryons in nuclear medium, as well as $\Lambda_c^+, \Sigma_c, \Xi_c$ and Λ_b hypernuclei. We hope that the present study inspires some interests for studying the properties of heavy baryons in nuclear medium at facilities like JHF, and particularly at RHIC, high energy relativistic heavy ion facility, and in very high energy experiments at CERN and Fermilab.

The organization of this article is as follows. In Section 2, the relativistic formulation of the charmed and bottom hypernuclear system in the QMC model will be explained. A mean-field Lagrangian density and equations of motion will be given in Section 2.1. Charmed and bottom hadrons in nuclear matter will be discussed in Section 2.2, while charmed and bottom hypernuclei will be treated in Section 2.3. In Section 3, the effects necessary for a realistic calculation of the heavy baryon hypernuclei will be described. Spin-orbit potential in the QMC model will be explained in Sections 3.1, while the effect of the Pauli blocking originating from the underlying quark structure of baryons, as well as the $\Sigma_{c,b}N - \Lambda_{c,b}N$ channel coupling effect will be explained in Section 3.2. The results calculated for the charmed and bottom hypernuclei will be presented in Section 4, and finally Section 5 will be devoted to summary and discussion.

2 Charmed and bottom hypernuclei in the QMC model

In this Section, we explain the mean-field equations of motion for a charmed or bottom hypernuclear system, and also discuss the properties of the charmed and bottom baryons in nuclear matter.

2.1 Mean-field equations of motion

Let us consider static, approximately spherically symmetric charmed and bottom hypernuclei, i.e., closed shell nuclear core plus one charmed or one bottom baryon (heavy baryon) configuration, ignoring small non-spherical effects due to the embedded heavy baryon. In principle, the existence of the heavy baryon inside or outside of the nuclear core breaks spherical symmetry, and one should include this effect in a truly rigorous treatment. We have neglected this effect, since it is expected to be of little importance for spectroscopic calculations [35, 36]. However, we include the response of the nuclear core arising from the self-consistent calculation, which is significant for a description of the baryon currents and magnetic moments, and a purely relativistic effect [36, 37]. Thus, we always specify the state of the heavy baryon in which the calculation is performed, because of the state dependent response of the core nucleus due to the self-consistency.

In addition, we adopt the Hartree, mean-field, approximation. In this approximation the ρNN tensor coupling gives a spin-orbit force for a nucleon bound in a static spherical nucleus, although in Hartree-Fock it can give a central force which contributes to the bulk symmetry energy [11, 12]. (Furthermore, it gives no contribution for nuclear matter since the meson fields are independent of position and time.) Thus, we ignore the ρNN tensor coupling in this study as applied in the study of hypernuclei [9], and usually adopted in the Hartree treatment of QHD [34].

Using the Born-Oppenheimer approximation, a relativistic Lagrangian density which gives the same mean-field equations of motion for a charmed or a bottom hypernucleus, in which the quasi-particles moving in single-particle orbits are three-quark clusters with the quantum numbers of a charmed or a bottom heavy baryon, or a nucleon, when expanded to the same order in velocity, is given by the QMC model [9, 11, 12]:

$$\begin{aligned}
\mathcal{L}_{QMC}^{CHY} &= \mathcal{L}_{QMC} + \mathcal{L}_{QMC}^C, \\
\mathcal{L}_{QMC} &= \bar{\psi}_N(\vec{r}) \left[i\gamma \cdot \partial - M_N^*(\sigma) - (g_\omega \omega(\vec{r}) + g_\rho \frac{\tau_3^N}{2} b(\vec{r}) + \frac{e}{2}(1 + \tau_3^N) A(\vec{r})) \gamma_0 \right] \psi_N(\vec{r}) \\
&\quad - \frac{1}{2} [(\nabla \sigma(\vec{r}))^2 + m_\sigma^2 \sigma(\vec{r})^2] + \frac{1}{2} [(\nabla \omega(\vec{r}))^2 + m_\omega^2 \omega(\vec{r})^2] \\
&\quad + \frac{1}{2} [(\nabla b(\vec{r}))^2 + m_\rho^2 b(\vec{r})^2] + \frac{1}{2} (\nabla A(\vec{r}))^2, \\
\mathcal{L}_{QMC}^C &= \sum_{\substack{C=\Lambda_c^+, \Sigma_c^0, +, ++, \\ \Xi_c^{0,+}, \Lambda_b}} \bar{\psi}_C(\vec{r}) \left[i\gamma \cdot \partial - M_C^*(\sigma) - (g_\omega^C \omega(\vec{r}) + g_\rho^C I_3^C b(\vec{r}) + e Q_C A(\vec{r})) \gamma_0 \right] \psi_C(\vec{r}),
\end{aligned} \tag{1}$$

where $\psi_N(\vec{r})$ ($\psi_C(\vec{r})$) and $b(\vec{r})$ are respectively the nucleon (charmed or bottom baryon) and the ρ meson (the time component in the third direction of isospin) fields, while m_σ , m_ω and m_ρ are the masses of the σ , ω and ρ meson fields. g_ω and g_ρ are the ω - N and ρ - N coupling constants which are related to the corresponding (u, d) -quark- ω , g_ω^q , and (u, d) -quark- ρ , g_ρ^q ,

coupling constants as $g_\omega = 3g_\omega^q$ and $g_\rho = g_\rho^q$ [11, 12]. Note that these meson fields, σ, ω and ρ , represent the quantum numbers and Lorentz structure which mediate the interactions among the nucleons in nuclear medium as in original QHD [34], corresponding, $\sigma \leftrightarrow \phi_0$, $\omega \leftrightarrow V_0$ and $b \leftrightarrow b_0$, and they may not necessarily be connected with the physical particles, nor quark model states. Their masses in nuclear medium do not vary in the present treatment of using QMC-I. Hereafter we will use notations for the quark flavors, $q \equiv u, d$ and $Q \equiv s, c, b$, as well as a terminology, “heavy baryon”, for the low-lying charmed baryons, $\Lambda_c^+, \Sigma_c^{0,+}, \Xi_c^{0,+}$ or a bottom baryon Λ_b , otherwise explicitly stated.

In an approximation where the σ , ω and ρ fields couple only to the u and d quarks, the coupling constants for the heavy baryon are obtained as $g_\omega^C = (n_q/3)g_\omega$, and $g_\rho^C \equiv g_\rho = g_\rho^q$, with n_q being the total number of valence u and d light quarks in the heavy baryon C . I_3^C and Q_C are the third component of the heavy baryon isospin operator and its electric charge in units of the proton charge, e , respectively. The field dependent σ - N and σ - C coupling strengths predicted by the QMC model, $g_\sigma(\sigma) \equiv g_\sigma^N(\sigma)$ and $g_\sigma^C(\sigma)$, related to the Lagrangian density of Eq. (1) at the hadronic level, are defined by

$$M_N^*(\sigma) \equiv M_N - g_\sigma(\sigma)\sigma(\vec{r}), \quad (2)$$

$$M_C^*(\sigma) \equiv M_C - g_\sigma^C(\sigma)\sigma(\vec{r}), \quad (3)$$

where M_N (M_C) is the free nucleon (heavy baryon) mass. Note that the dependence of these coupling strengths on the applied scalar field must be calculated self-consistently within the quark model [9, 11, 12]. Hence, unlike QHD [34], even though $g_\sigma^C(\sigma)/g_\sigma(\sigma)$ may be $2/3$ or $1/3$ depending on the number of light quarks in the heavy baryon in free space ($\sigma = 0$)¹, this will not necessarily be the case in nuclear matter. Explicit expressions for $g_\sigma^C(\sigma)$ and $g_\sigma(\sigma)$ will be given later in Eq. (14). From the Lagrangian density Eq. (1), a set of equations of motion for the heavy baryon hypernuclear system is obtained:

$$[i\gamma \cdot \partial - M_N^*(\sigma) - (g_\omega\omega(\vec{r}) + g_\rho\frac{\tau_3^N}{2}b(\vec{r}) + \frac{e}{2}(1 + \tau_3^N)A(\vec{r}))\gamma_0]\psi_N(\vec{r}) = 0, \quad (4)$$

$$[i\gamma \cdot \partial - M_C^*(\sigma) - (g_\omega^C\omega(\vec{r}) + g_\rho^CI_3^C b(\vec{r}) + eQ_C A(\vec{r}))\gamma_0]\psi_C(\vec{r}) = 0, \quad (5)$$

$$(-\nabla_r^2 + m_\sigma^2)\sigma(\vec{r}) = -[\frac{\partial M_N^*(\sigma)}{\partial \sigma}]\rho_s(\vec{r}) - [\frac{\partial M_C^*(\sigma)}{\partial \sigma}]\rho_s^C(\vec{r}), \\ \equiv g_\sigma C_N(\sigma)\rho_s(\vec{r}) + g_\sigma^C C_C(\sigma)\rho_s^C(\vec{r}), \quad (6)$$

$$(-\nabla_r^2 + m_\omega^2)\omega(\vec{r}) = g_\omega\rho_B(\vec{r}) + g_\omega^C\rho_B^C(\vec{r}), \quad (7)$$

$$(-\nabla_r^2 + m_\rho^2)b(\vec{r}) = \frac{g_\rho}{2}\rho_3(\vec{r}) + g_\rho^CI_3^C\rho_B^C(\vec{r}), \quad (8)$$

$$(-\nabla_r^2)A(\vec{r}) = e\rho_p(\vec{r}) + eQ_C\rho_B^C(\vec{r}), \quad (9)$$

where, $\rho_s(\vec{r})$ ($\rho_s^C(\vec{r})$), $\rho_B(\vec{r})$ ($\rho_B^C(\vec{r})$), $\rho_3(\vec{r})$ and $\rho_p(\vec{r})$ are the scalar, baryon, third component of isovector, and proton densities at the position \vec{r} in the heavy baryon hypernucleus [9, 11, 12]. On the right hand side of Eq. (6), $-[\partial M_N^*(\sigma)/\partial \sigma] \equiv g_\sigma C_N(\sigma)$ and $-[\partial M_C^*(\sigma)/\partial \sigma] \equiv g_\sigma^C C_C(\sigma)$, where $g_\sigma \equiv g_\sigma(\sigma = 0)$ and $g_\sigma^C \equiv g_\sigma^C(\sigma = 0)$, are a new, and characteristic feature of QMC beyond QHD [34, 39, 40, 41]. The effective mass for the heavy baryon C is defined by

$$\frac{\partial M_C^*(\sigma)}{\partial \sigma} = -n_q g_\sigma^q \int_{bag} d^3x \bar{\psi}_q(\vec{x})\psi_q(\vec{x}) \equiv -n_q g_\sigma^q S_C(\sigma) = -\frac{\partial}{\partial \sigma} [g_\sigma^C(\sigma)\sigma], \quad (10)$$

¹Strictly, this is true only when the bag radii of nucleon and heavy baryon C are exactly the same in the present model. See Eq. (12) - (14).

with the MIT bag model quantities, and the mass stability condition to be satisfied in obtaining the in-medium bag radius [2, 9, 11, 12]:

$$M_C^*(\sigma) = \sum_{j=q,Q} \frac{n_j \Omega_j^* - z_C}{R_C^*} + \frac{4}{3} \pi (R_C^*)^3 B, \quad (11)$$

$$S_C(\sigma) = \frac{\Omega_q^*/2 + m_q^* R_C^* (\Omega_q^* - 1)}{\Omega_q^* (\Omega_q^* - 1) + m_q^* R_C^*/2}, \quad (12)$$

$$\Omega_q^* = \sqrt{x_q^2 + (R_C^* m_q^*)^2}, \quad \Omega_Q^* = \sqrt{x_Q^2 + (R_C^* m_Q)^2}, \quad m_q^* = m_q - g_\sigma^q \sigma(\vec{r}), \quad (13)$$

$$C_C(\sigma) = S_C(\sigma)/S_C(0), \quad g_\sigma^C \equiv n_q g_\sigma^q S_C(0) \equiv \frac{n_q}{3} g_\sigma \Gamma_{C/N} = \frac{n_q}{3} g_\sigma S_C(0)/S_N(0), \quad (14)$$

$$\left. \frac{dM_C^*}{dR_C} \right|_{R_C=R_C^*} = 0. \quad (15)$$

Quantities for the nucleon are similarly obtained by replacing the indices, $C \rightarrow N$, in Eqs. (10) - (15). The MIT bag model quantities for the heavy baryon C , are calculated in a local density approximation, using the spin and spatial part of the wave functions for a quark flavor f , $\psi_f(x) = N_f e^{-i\epsilon_f t/R_C^*} \psi_f(\vec{x})$, with N_f being the normalization factor. The wave functions, $\psi_f(x)$, satisfy the Dirac equations for the quarks in the baryon bag centered at a position \vec{r} of the nucleus, approximating the constant, mean meson fields within the bag neglecting the Coulomb force ($|\vec{x} - \vec{r}| \leq$ bag radius [15, 16, 20]):

$$\left[i\gamma \cdot \partial_x - (m_q - V_\sigma^q(\vec{r})) - \gamma^0 \left(V_\omega^q(\vec{r}) \pm \frac{1}{2} V_\rho^q(\vec{r}) \right) \right] \begin{pmatrix} \psi_u(x) \\ \psi_d(x) \end{pmatrix} = 0, \quad (16)$$

$$[i\gamma \cdot \partial_x - m_Q] \psi_Q(x) = 0, \quad (17)$$

where, $q = u$ or d , and $Q = s, c$ or b . The constant, mean-field potentials within the bag are defined by $V_\sigma^q(\vec{r}) \equiv g_\sigma^q \sigma(\vec{r})$, $V_\omega^q(\vec{r}) \equiv g_\omega^q \omega(\vec{r})$ and $V_\rho^q(\vec{r}) \equiv g_\rho^q b(\vec{r})$, with g_σ^q , g_ω^q and g_ρ^q the corresponding quark-meson coupling constants. The eigenenergies, $\epsilon_{u,d,Q}$ in units of $1/R_C^*$ are given by

$$\begin{pmatrix} \epsilon_u \\ \epsilon_d \end{pmatrix} = \Omega_q^* + R_C^* \left(V_\omega^q(\vec{r}) \pm \frac{1}{2} V_\rho^q(\vec{r}) \right), \quad \epsilon_Q = \Omega_Q^*, \quad (18)$$

where, Ω_q^* and Ω_Q^* are given in Eq. (13).

In the expressions of the MIT bag quantities Eqs. (11) and (13), z_C , B , $x_{q,Q}$, and $m_{q,Q}$ are the parameters for the sum of the c.m. and gluon fluctuation effects, bag pressure, lowest eigenvalues for the quarks q or Q , respectively, and the corresponding current quark masses. z_N and B (z_C) are fixed by fitting the nucleon (heavy baryon) mass in free space. For the current quark masses, we use, $(m_{u,d}, m_s, m_c, m_b) = (5, 250, 1300, 4200)$ MeV, and obtain the bag pressure, $B = (170 \text{ MeV})^4$, by choosing the bag radius for the nucleon in free space, $R_N = 0.8 \text{ fm}$. The quark-meson coupling constants, which are determined so as to reproduce the saturation properties of symmetric nuclear matter, are, $(g_\sigma^q, g_\omega^q, g_\rho^q) = (5.69, 2.72, 9.33)$, where $g_\sigma \equiv g_\sigma^N \equiv 3g_\sigma^q S_N(0) = 3 \times 5.69 \times 0.483 = 8.23$ [12]. (See Eq. (14) with the replacement, $C \rightarrow N$.) The parameters z_j , and the bag radii R_j in free space ($j = N, \Lambda, \Sigma, \Xi, \Lambda_c^+, \Sigma_c, \Xi_c, \Lambda_b$) and also some quantities calculated at normal nuclear matter density $\rho_B = 0.15 \text{ fm}^{-3}$, are listed in Table 1, together with the free space masses [38] used for the calculation. (Nuclear matter limit will be discussed in Section 2.2.) Concerning the sign of m_q^* in hypernucleus in Eq. (13),

it reflects nothing but the strength of the attractive scalar potential which is usually negative for a particle tightly bound, and thus naive interpretation of the mass for a physical particle, which is positive, should not be applied.

Table 1: The bag parameters, the baryon masses and the bag radii in free space [at normal nuclear matter density, $\rho_B = 0.15 \text{ fm}^{-3}$] z_j , R_j and M_j [R_j^* and M_j^*] ($j = N, \Lambda, \Lambda_c^+, \Sigma_c, \Xi_c, \Lambda_b$), respectively. They are obtained with the bag pressure, $B = (170 \text{ MeV})^4$, and current quark masses, $(m_{u,d}, m_s, m_c, m_b) = (5, 250, 1300, 4200) \text{ MeV}$, together with the quark-meson coupling constants, $(g_\sigma^q, g_\omega^q, g_\rho^q) = (5.69, 2.72, 9.33)$, where $g_\sigma \equiv g_\sigma^N = 3g_\sigma^q S_N(0) = 3 \times 5.69 \times 0.483 = 8.23$ [12]. Quantities for the strange hyperons are taken from Ref. [9].

j	z_j	M_j (MeV)	R_j (fm)	M_j^* (MeV)	R_j^* (fm)
N	3.295	939.0	0.800	754.5	0.786
Λ	3.131	1115.7	0.806	992.7	0.803
Σ	2.810	1193.1	0.827	1070.4	0.824
Ξ	2.860	1318.1	0.820	1256.7	0.818
Λ_c^+	1.766	2284.9	0.846	2162.5	0.843
Σ_c	1.033	2452.0	0.885	2330.2	0.882
Ξ_c	1.564	2469.1	0.853	2408.0	0.851
Λ_b	-0.643	5624.0	0.930	5502.9	0.928

At the hadronic level, the entire information on the quark dynamics is condensed into the effective couplings $C_{N,C}(\sigma)$ of Eq. (6). Furthermore, when $C_{N,C}(\sigma) = 1$, which corresponds to a structureless nucleon or a heavy baryon, the equations of motion given by Eqs. (4) - (9) can be identified with those derived from QHD [39, 40, 41], except for the terms arising from the tensor coupling and the non-linear scalar and/or vector field interactions introduced beyond naive QHD.

2.2 Nuclear matter limit

Let us consider a limit of nuclear matter and discuss briefly properties of heavy baryons in the nuclear medium. In this limit all meson fields become constant, and we denote the mean-values of the ω and σ fields by $\bar{\omega}$ and $\bar{\sigma}$, respectively. Then, equations for the $\bar{\omega}$ and self-consistency condition for the $\bar{\sigma}$ are given by [2, 11, 12, 13]

$$\bar{\omega} = \frac{4}{(2\pi)^3} \int d^3k \theta(k_F - k) = \frac{g_\omega}{m_\omega^2} \frac{2k_F^3}{3\pi^2} = \frac{g_\omega}{m_\omega^2} \rho_B, \quad (19)$$

$$\bar{\sigma} = \frac{g_\sigma}{m_\sigma^2} C_N(\bar{\sigma}) \frac{4}{(2\pi)^3} \int d^3k \theta(k_F - k) \frac{M_N^*(\bar{\sigma})}{\sqrt{M_N^{*2}(\bar{\sigma}) + \vec{k}^2}} = \frac{g_\sigma}{m_\sigma^2} C_N(\bar{\sigma}) \rho_s, \quad (20)$$

where $g_\sigma = 3g_\sigma^q S_N(0)$ (see Eq. (14) by the replacement, $C \rightarrow N$), k_F is the Fermi momentum, ρ_B and ρ_s are the baryon and scalar densities, respectively. Note that $M_N^*(\bar{\sigma})$ in Eq. (20), must be calculated self-consistently by the MIT bag model, through Eqs. (10) - (16). This self-consistency equation for the $\bar{\sigma}$ is the same as that in QHD, except that in the latter one

has $C_N(\bar{\sigma}) = 1$ [34]. Using the mean field value $\bar{\sigma}$, the corresponding quantity for the heavy baryon C , $C_C(\bar{\sigma})$, can be also calculated using Eqs. (10) - (17) neglecting the effect of a single heavy baryon on the mean field value $\bar{\sigma}$, in infinite nuclear matter.

It has been found that the function $C_j(\bar{\sigma})(j = N, \Lambda, \Sigma, \Xi, \Lambda_c^+, \Sigma_c, \Xi_c, \Lambda_b)$ can be parametrized as a linear form in the σ field, $g_\sigma \bar{\sigma}$, for practical calculations [9, 11, 12]:

$$C_j(\bar{\sigma}) = 1 - a_j \times (g_\sigma \bar{\sigma}), \quad (j = N, \Lambda, \Sigma, \Xi, \Lambda_c^+, \Sigma_c, \Xi_c, \Lambda_b). \quad (21)$$

The values obtained for a_j are listed in Table 2. This parametrization works very well up to about three times of normal nuclear matter density $\rho_B \simeq 3\rho_0$, with $\rho_0 \simeq 0.15 \text{ fm}^{-3}$. Then, the effective masses for the baryon, j , in nuclear matter is well approximated by [9, 11, 12]

$$M_j^\star \simeq M_j - \frac{n_q}{3} g_\sigma \left[1 - \frac{a_j}{2} (g_\sigma \bar{\sigma}) \right] \bar{\sigma}, \quad (j = N, \Lambda, \Sigma, \Xi, \Lambda_c^+, \Sigma_c, \Xi_c, \Lambda_b), \quad (22)$$

with n_q being the number of light quarks in the baryon j . For the field strength $g_\sigma \bar{\sigma}$ versus baryon density, see Ref. [11].

Table 2: The slope parameters, a_j ($j = N, \Lambda, \Sigma, \Xi, \Lambda_c^+, \Sigma_c, \Xi_c, \Lambda_b$).

a_j	$\times 10^{-4} \text{ MeV}^{-1}$	a_j	$\times 10^{-4} \text{ MeV}^{-1}$
a_N	8.8	a_{Λ_b}	10.9
a_Λ	9.3	$a_{\Lambda_c^+}$	9.8
a_Σ	9.5	a_{Σ_c}	10.3
a_Ξ	9.4	a_{Ξ_c}	9.9

In Fig. 1 we show the calculated ratios of effective masses versus those of the free particles in nuclear matter. With increasing density the ratios decrease as usually expected, but decrease in magnitude is from larger to smaller except for Ξ : baryons with only light quarks, with one strange quark, with one charm quark, and with one bottom quark. This is because their masses (except for Ξ) in free space are in the reverse order from light to heavy. Thus, the net ratios for the decrease in masses (developing of scalar potentials) compared to that of the free masses becomes smaller. This may be regarded as a measure of the role of light quarks in each baryon in nuclear matter, in a sense that by how much ratio they lead to a partial restoration of chiral symmetry in the baryon.

It is more quantitative and direct to compare the scalar and vector potentials of baryons in nuclear matter. The scalar (V_s^B) and vector (V_v^B) potentials for the baryon B , in nuclear matter are given by

$$V_s^B = m_B^\star - m_B, \quad (23)$$

$$V_v^B = (n_q - n_{\bar{q}}) V_\omega^q + I_3^B V_\rho^q, \quad (24)$$

where I_3^B is the third component of isospin projection of the baryon B . Thus, the vector potential for a heavy baryon with charm or bottom quarks, is equal to that of the hyperon with the same light quark number in the QMC model. Calculated results for the scalar potentials

for the baryons are shown in Fig. 2. From the results it is confirmed that the scalar potential for the baryon B , V_s^B , follows a simple light quark number counting rule:

$$V_s^B \simeq \frac{n_q}{3} V_s^N, \quad (25)$$

where n_q is the number of light quarks in the baryon B , and V_s^N is the scalar potential for the nucleon. (See Eq.(23).) It is interesting to notice that, the baryons with charm and bottom quarks (Ξ_c is a quark flavor configuration, qsc), show very similar features to those of the corresponding strange hyperons with the same light quark numbers. Then, ignoring the Coulomb force although it is important in a realistic hypernucleus, we may expect that these heavy baryons with charm or bottom quarks, will also form some heavy baryon hypernuclei at this stage, as the strange hyperons do. (Recall that the repulsive, vector potentials are the same for the corresponding hyperons with the same light quark numbers.)

2.3 Charmed and bottom hypernuclei

We give here the explicit expressions for coupled differential equations to obtain various fields and baryon wave functions to describe a heavy baryon hypernuclear system. The variation of the Lagrangian density Eq. (1) results in the following equations for static, spherically symmetric nucleus plus one heavy baryon configuration—a heavy baryon hypernucleus:

$$\frac{d^2}{dr^2}\sigma(r) + \frac{2}{r} \frac{d}{dr}\sigma(r) - m_\sigma^2\sigma(r) = -g_\sigma C_N(\sigma(r))\rho_s(r) - g_\sigma^C C_C(\sigma(r))\rho_s^C(r), \quad (26)$$

$$\frac{d^2}{dr^2}\omega(r) + \frac{2}{r} \frac{d}{dr}\omega(r) - m_\omega^2\omega(r) = -g_\omega\rho_B(r) - g_\omega^C\rho_B^C(r), \quad (27)$$

$$\frac{d^2}{dr^2}b(r) + \frac{2}{r} \frac{d}{dr}b(r) - m_\rho^2b(r) = -\frac{g_\rho}{2}\rho_3(r) - g_\rho^C t_\beta\rho_B^C(r), \quad (28)$$

$$\frac{d^2}{dr^2}A(r) + \frac{2}{r} \frac{d}{dr}A(r) = -e\rho_p(r) - eQ_C\rho_B^C(r), \quad (29)$$

(30)

where

$$\rho_s(r) = \sum_{\alpha}^{occ} d_{\alpha}(r)(|G_{\alpha}(r)|^2 - |F_{\alpha}(r)|^2), \quad (31)$$

$$\rho_s^C(r) = d_{\beta}(r)(|G_{\beta}(r)|^2 - |F_{\beta}(r)|^2), \quad (32)$$

$$\rho_B(r) = \sum_{\alpha}^{occ} d_{\alpha}(r)(|G_{\alpha}(r)|^2 + |F_{\alpha}(r)|^2), \quad (33)$$

$$\rho_B^C(r) = d_{\beta}(r)(|G_{\beta}(r)|^2 + |F_{\beta}(r)|^2), \quad (34)$$

$$\rho_3(r) = \sum_{\alpha}^{occ} d_{\alpha}(r)(-)^{t_{\alpha}-1/2}(|G_{\alpha}(r)|^2 + |F_{\alpha}(r)|^2), \quad (35)$$

$$\rho_p(r) = \sum_{\alpha}^{occ} d_{\alpha}(r)(t_{\alpha} + \frac{1}{2})(|G_{\alpha}(r)|^2 + |F_{\alpha}(r)|^2), \quad (36)$$

with $d_{\alpha}(r) = (2j_{\alpha} + 1)/4\pi r^2$, $d_{\beta}(r) = 1/4\pi r^2$ and

$$\frac{d}{dr}G_{\alpha}(r) + \frac{\kappa}{r}G_{\alpha}(r) - [\epsilon_{\alpha} - g_{\omega}\omega(r) - t_{\alpha}g_{\rho}b(r) - (t_{\alpha} + \frac{1}{2})eA(r) + M_N$$

$$- g_\sigma(\sigma(r))\sigma(r)] F_\alpha(r) = 0, \quad (37)$$

$$\begin{aligned} \frac{d}{dr} F_\alpha(r) - \frac{\kappa}{r} F_\alpha(r) + [\epsilon_\alpha - g_\omega \omega(r) - t_\alpha g_\rho b(r) & - (t_\alpha + \frac{1}{2}) e A(r) - M_N \\ & + g_\sigma(\sigma(r))\sigma(r)] G_\alpha(r) = 0, \end{aligned} \quad (38)$$

$$\begin{aligned} \frac{d}{dr} G_\beta(r) + \frac{\kappa}{r} G_\beta(r) - [\epsilon_\beta - g_\omega^C \omega(r) - t_\beta g_\rho^C b(r) & - e Q_C A(r) + M_C \\ & - g_\sigma^C(\sigma(r))\sigma(r)] F_\beta(r) = 0, \end{aligned} \quad (39)$$

$$\begin{aligned} \frac{d}{dr} F_\beta(r) - \frac{\kappa}{r} F_\beta(r) + [\epsilon_\beta - g_\omega^C \omega(r) - t_\beta g_\rho^C b(r) & - e Q_C A(r) - M_C \\ & + g_\sigma^C(\sigma(r))\sigma(r)] G_\beta(r) = 0. \end{aligned} \quad (40)$$

Here $G_{\alpha,\beta}(r)/r$ and $F_{\alpha,\beta}(r)/r$ are respectively the radial part of the upper and lower components of the solution to the Dirac equation for the nucleon (heavy baryon C) [34]:

$$\psi_{N,C}(\vec{r}) = \begin{pmatrix} i[G_{\alpha,\beta}(r)/r]\Phi_{\kappa m} \\ -[F_{\alpha,\beta}(r)/r]\Phi_{-\kappa m} \end{pmatrix} \xi_{t_{\alpha,\beta}}, \quad (41)$$

where $\xi_{t_{\alpha,\beta}}$ is an isospin part of the wave function, and $\Phi_{\kappa m}$ is a spin spherical harmonic for the nucleon (heavy baryon) [12, 9] (α (β) labeling the quantum numbers of nucleon (heavy baryon) and $\epsilon_{\alpha,\beta}$ being the corresponding energies). Then, the normalization condition is given by

$$\int dr(|G_{\alpha,\beta}(r)|^2 + |F_{\alpha,\beta}(r)|^2) = 1. \quad (42)$$

As usual, κ specifies the angular quantum numbers and t_α (t_β) the eigenvalue of the isospin operator $\tau_3^N/2$ (I_3^C). The total energy of the heavy baryon hypernuclear system is then given by

$$\begin{aligned} E_{tot} = \sum_{\alpha}^{occ} (2j_\alpha + 1) \epsilon_\alpha + \epsilon_\beta - \frac{1}{2} \int d\vec{r} [-g_\sigma C_N(\sigma(r))\sigma(r)\rho_s(r) \\ + g_\omega \omega(r)\rho_B(r) + \frac{1}{2} g_\rho b(r)\rho_3(r) + e A(r)\rho_p(r)] \\ - \frac{1}{2} \int d\vec{r} [-g_\sigma^C C_C(\sigma(r))\sigma(r)\rho_s^C(r) \\ + g_\omega^C \omega(r)\rho_B^C(r) + g_\rho^C b(r)t_\beta \rho_B^C(r) + e Q_C A(r)\rho_B^C(r)]. \end{aligned} \quad (43)$$

3 Calculation

In this section, we discuss parameters used in the calculation of heavy baryon hypernuclei, spin-orbit force in the QMC model, Pauli blocking effect at the quark level, and the effect of channel coupling, $\Sigma_{c,b}N - \Lambda_{c,b}N$.

3.1 Spin-orbit force in the QMC model

The origin of the spin orbit force for a composite nucleon moving through scalar and vector fields which vary with position is explained in detail in Ref. [11]. The detailed discussion for the Λ , Σ

and Ξ is given in Ref. [9]. Although the spin-orbit splittings for the nucleon calculated in QMC are already somewhat smaller [11, 12] than those calculated in QHD [34], it was demonstrated that much smaller spin-orbit splittings were obtained for the Λ in QMC [9], and it will turn out to be even smaller for the heavy baryon hypernuclei.

In order to include the spin-orbit potential approximately, e.g., for the Λ_c^+ , we add perturbatively the correction due to the vector potential, $-\frac{2}{2M_{\Lambda_c^+}^{*2}(\vec{r})r} \left(\frac{d}{dr} g_{\omega}^{\Lambda_c^+} \omega(\vec{r}) \right) \vec{l} \cdot \vec{s}$, to the single-particle energies obtained with the Dirac equation, in the same way as that added for the strange hypernuclei in Ref. [9]. This may correspond to a correct spin-orbit force which is calculated by the underlying quark model [9, 11]:

$$V_{S.O.}^{\Lambda_c^+}(\vec{r}) \vec{l} \cdot \vec{s} = -\frac{1}{2M_{\Lambda_c^+}^{*2}(\vec{r})r} \left(\frac{d}{dr} [M_{\Lambda_c^+}^*(\vec{r}) + g_{\omega}^{\Lambda_c^+} \omega(\vec{r})] \right) \vec{l} \cdot \vec{s}, \quad (44)$$

since the Dirac equation at the hadronic level solved in usual QHD-type models leads to:

$$V_{S.O.}^{\Lambda_c^+}(\vec{r}) \vec{l} \cdot \vec{s} = -\frac{1}{2M_{\Lambda_c^+}^{*2}(\vec{r})r} \left(\frac{d}{dr} [M_{\Lambda_c^+}^*(\vec{r}) - g_{\omega}^{\Lambda_c^+} \omega(\vec{r})] \right) \vec{l} \cdot \vec{s}, \quad (45)$$

which has the opposite sign for the vector potential, $g_{\omega}^{\Lambda_c^+} \omega(\vec{r})$. The correction to the spin-orbit force, which appears naturally in the QMC model, may also be modeled at the hadronic level of the Dirac equation by adding a tensor interaction, motivated by the quark model [42, 43]. Here, we should make a comment that, as was discussed by Dover and Gal [44] in detail, one boson exchange model with underlying approximate SU(3) symmetry in strong interactions, also leads to a weaker spin-orbit forces for the (strange) hyperon-nucleon (YN) than that for the nucleon-nucleon (NN).

However, in practice, because of its heavy mass ($M_{\Lambda_c^+}^*$), contribution to the single-particle energies from the spin-orbit potential both with or without the inclusion of the correction term, turns out to be even smaller than that for the Λ hypernuclei, and further smaller for the Λ_b hypernuclei [8]. Contribution from the spin-orbit potential with the correction term is typically of order 0.01 MeV, and even for the largest case is $\simeq 0.5$ MeV, among the all heavy baryon hypernuclei calculated in this study. This can be understood when one considers the limit, $M_{\Lambda_c^+}^* \rightarrow \infty$ in Eq. (44), where the quantity inside the square brackets varies smoothly from an order of hundred MeV to zero near the surface of the hypernucleus, and the derivative with respect to r is finite. The situations for the other heavy baryon hypernuclei are very similar, and spin-orbit forces give only tiny contributions for the single-particle energies.

3.2 Effects of the Pauli blocking and channel coupling

In this section, we explain briefly the effects of the Pauli blocking originating from the underlying quark structure, and the channel coupling. Detail description is given in Ref. [9].

Although the present treatment is based on the underlying quark structure of the nucleon and heavy baryons, it is missing an explicit inclusion of the Pauli blocking effect at the quark level among the u and d quarks in the core nucleons and the heavy baryons. For the strange hypernuclei, the effect of the Pauli blocking was included in a specific way at the hadronic level. We follow the treatment of Ref. [9], and include effective Pauli blocking and also the $\Sigma_{c,b}N - \Lambda_{c,b}N$ channel coupling effects, although the channel coupling effect is expected to be

smaller than that for the $\Sigma N - \Lambda N$, since the mass difference for the former is larger than the latter. Thus, the channel coupling effect which we include for the Σ_c hypernuclei in the present study should be regarded in order to ensure the limiting case. The channel coupling effect is significant in the open, coupled channel, particularly in the $\Sigma N - \Lambda N$ channel, where such phenomenon simply does not occur for two nucleons in the core nucleus. This effect may be also one of the reasons why no narrow states have been found for the Σ hypernuclei experimentally.

In Ref. [9], it was assumed that this effect works repulsively in a way that the strength is proportional to the u and/or d quark baryonic density of the core nucleons. Then one can expect that the u and/or d quarks in the heavy baryon feel a stronger repulsion at the position where the baryon density is large. As a consequence, the wave function of the heavy baryon (light quark) will be suppressed in this region. We assume here in the same way that the Pauli blocking effect is simply proportional to the nucleon baryonic density (or u and d total light quark number density) [9], although one could consider a more complicated density dependence. Then, the Dirac equation for the heavy baryon C , Eq. (5), may be modified by

$$[i\gamma \cdot \partial - M_C^*(\sigma) - (\lambda_C \rho_B(\vec{r}) + g_\omega^C \omega(\vec{r}) + g_\rho I_3^C b(\vec{r}) + e Q_C A(\vec{r})) \gamma_0] \psi_C(\vec{r}) = 0, \quad (46)$$

where, $\rho_B(\vec{r})$ is the baryonic density at the position \vec{r} in the heavy baryon hypernucleus due to the core nucleons, and λ_C is a constant to be taken the same value to that determined for the strange hyperon. We note that the Pauli blocking effect associated with the light quarks in the heavy baryon should also lead to some repulsion for the nucleons. Contrary to the comment made in Ref. [9], it turned out that the actual calculation there included the effect of the modification made in Eq. (46) in a self-consistent manner, as those included for the total baryon and scalar densities and the vector and scalar potentials. Thus, the response of the core nucleons due to the modification in Eq. (46), were included in Ref. [8, 9], and is also included in this study.

For the Λ hypernuclei [9] the parameter corresponding to λ_C in Eq. (46) was chosen to reproduce the empirical single particle energy for the $1s_{1/2}$ in $^{209}\Lambda\text{Pb}$, -27.0 MeV [46]. The fitted value for the constant was, $\lambda_\Lambda = 60.25 \text{ MeV (fm)}^3$. Thus, we use the same value also for the $\Lambda_{c,b}$, i.e., $\lambda_{\Lambda_{c,b}} = 60.25 \text{ MeV (fm)}^3$. For the Σ_c and Ξ_c hypernuclei, we can deduce the constants $\lambda_{\Sigma_c, \Xi_c}$, corresponding to the effective Pauli blocking effect as, $\lambda_{\Sigma_c} = \lambda_{\Lambda_c}$, and $\lambda_{\Xi_c} = \frac{1}{2}\lambda_{\Lambda_c}$, by counting the total number of u and d quarks in the heavy baryons.

One may regard that this fitted value for the Λ , thus, for the $\Lambda_{c,b}$ hypernuclei, includes also the attractive $\Lambda_{c,b}N \rightarrow \Sigma_{c,b}N$ channel coupling effect for the $\Lambda_{c,b}$ single-particle energies, because the value fitted for the Λ hypernuclei includes the experimentally observed effect of the $\Lambda N \rightarrow \Sigma N$ channel coupling. As for the $\Sigma_c N \rightarrow \Lambda_c N$ channel coupling effect, it must be included additionally to the effect for the $\Lambda_{c,b}$ to reproduce the relative repulsive energy shift in the single-particle energies for the Σ_c , as was done for the Σ hypernuclei.

The $\Sigma N - \Lambda N$ channel coupling was estimated using the Nijmegen potential in Ref. [9]. The effect for the Σ was included by assuming the same form as that was applied for the effective Pauli blocking via $\lambda_\Sigma \rho_B(r)$, and adjusted the parameter, $\lambda_\Sigma = \lambda_\Lambda \rightarrow \tilde{\lambda}_\Sigma \neq \lambda_\Sigma$, to reproduce this difference in the single-particle energy for the $1s_{1/2}$ in $^{209}\Sigma\text{Pb}$, namely, $-19.6 = -26.9 (\simeq -27.0) + 7.3 \text{ MeV}$. The value obtained for $\tilde{\lambda}_\Sigma$ in this way was, $\tilde{\lambda}_\Sigma = 110.6 \text{ MeV (fm)}^3$. Thus, we use the same value, $\tilde{\lambda}_{\Sigma_c} = 110.6 \text{ MeV (fm)}^3$, although we expect the effect should be smaller in considering the mass differences, $m_\Sigma - m_\Lambda \simeq 77 \text{ MeV}$ and $m_{\Sigma_c} - m_{\Lambda_c^+} \simeq 166 \text{ MeV}$ [38]. As for the $\Xi N - \Lambda\Lambda$ channel coupling the effect was estimated to be negligible in Ref. [9], and we also neglect the effect for Ξ_c in this study.

4 Results for heavy baryon hypernuclei

Before presenting the calculated results, we summarize in Table 3 the parameters at the hadronic level fixed by the saturation properties of symmetric nuclear matter and used in the calculation of heavy baryon hypernuclei. Concerning the parameters for the σ field, we note that the properties of nuclear matter only fix the ratio, (g_σ/m_σ) , with a chosen value, $m_\sigma = 550$ MeV. Keeping this ratio to be a constant, the value $m_\sigma = 418$ MeV for finite nuclei (hypernuclei) is obtained by fitting the r.m.s. charge radius of ^{40}Ca to the experimental value, $r_{\text{ch}}(^{40}\text{Ca}) = 3.48$ fm [12]. (See also Section 2.1 for the value of g_σ in nuclear matter.)

Table 3: Parameters at the hadronic level for finite nuclei [12].

field	mass (MeV)	$g^2/4\pi (e^2/4\pi)$
σ	418	3.12
ω	783	5.31
ρ	770	6.93
A	0	1/137.036

Now we are in a position to present the results. In Tables 4 and 5, we list the calculated single-particle energies for ${}_j^{\Lambda}\text{O}$, ${}_j^{\Lambda}\text{Ca}$, ${}_j^{\Lambda}\text{Ca}$, ${}_j^{\Lambda}\text{Zr}$ and ${}_j^{\Lambda}\text{Pb}$ ($j = \Lambda, \Lambda_c^+, \Sigma_c^{0,+,++}, \Xi_c^{0,+}, \Lambda_b$) hypernuclei, together with the experimental data [45, 46] for the Λ hypernuclei. In the calculation, we have searched for the single-particle states up to the same highest state as that of the core neutrons in each hypernucleus, since the deeper levels are usually easier to observe in experiment.

From the results shown in Tables 4 and 5 we notice:

1. Σ_c^{++} and Ξ_c^+ hypernuclei are very unlikely to be formed in usual circumstances. Solid conclusions may not be drawn about ${}_{\Sigma_c^{++}, \Xi_c^+}^{\Lambda}\text{Ca}$. Although results imply the formations of these hypernuclei, those numbers may be regarded within the ambiguities of the model and the approximations made in the calculation.
2. Σ_c^0 and Σ_c^+ hypernuclei may have some possibilities to be formed in considering the obtained single-particle energies. (Discussions on the Σ_c^0 hypernuclei will be given later.)
3. Λ_c^+, Ξ_c^0 and Λ_b hypernuclei are expected to be formed quite likely in a realistic situation. However, for the Λ_b hypernuclei, it will be very difficult to achieve such a resolution to distinguish the states experimentally.
4. The Coulomb force plays a crucial role in forming (unforming) hypernuclei, by comparing the single-particle energies among/between the members within each multiplet of hypernuclei, $(\Lambda, \Lambda_c^+, \Lambda_b)$, $(\Sigma_c^0, \Sigma_c^+, \Sigma_c^{++})$, and (Ξ_c^0, Ξ_c^+) hypernuclei.

We comment on the Σ_c^0 hypernuclei single-particle energies, which have a peculiar feature. In some of the hypernuclei calculated, the $1s_{1/2}$ state could not be found in the following sense. We have searched for the $1s_{1/2}$ state by varying matching point to get the eigenenergy and the corresponding eigen wave function for the Σ_c^0 in step 0.1 fm, from 0.2 fm to 5.0 fm from the

Table 4: Single-particle energies (in MeV) for $^{17}_j\text{O}$, $^{41}_j\text{Ca}$ and $^{49}_j\text{Ca}$ ($j = \Lambda, \Lambda_c^+, \Sigma_c, \Xi_c, \Lambda_b$), calculated with the effective Pauli blocking and the $\Sigma_{c,b}N - \Lambda_{c,b}N$ channel coupling. Experimental data are taken from Ref. [45]. Spin-orbit splittings for the Λ hypernuclei are not well determined by the experiments.

	$^{16}_\Lambda\text{O}$ (Exp.)	$^{17}_\Lambda\text{O}$	$^{17}_{\Lambda_c^+}\text{O}$	$^{17}_{\Sigma_c^0}\text{O}$	$^{17}_{\Sigma_c^+}\text{O}$	$^{17}_{\Sigma_c^{++}}\text{O}$	$^{17}_{\Xi_c^0}\text{O}$	$^{17}_{\Xi_c^+}\text{O}$	$^{17}_{\Lambda_b}\text{O}$
$1s_{1/2}$	-12.5	-14.1	-12.8	—	-7.5	—	-7.9	-2.1	-19.6
$1p_{3/2}$	-2.5 (1p)	-5.1	-7.3	-10.7	-4.0	—	-3.5	—	-16.5
$1p_{1/2}$	-2.5 (1p)	-5.0	-7.3	-10.2	-3.6	—	-3.5	—	-16.5
	$^{40}_\Lambda\text{Ca}$ (Exp.)	$^{41}_\Lambda\text{Ca}$	$^{41}_{\Lambda_c^+}\text{Ca}$	$^{41}_{\Sigma_c^0}\text{Ca}$	$^{41}_{\Sigma_c^+}\text{Ca}$	$^{41}_{\Sigma_c^{++}}\text{Ca}$	$^{41}_{\Xi_c^0}\text{Ca}$	$^{41}_{\Xi_c^+}\text{Ca}$	$^{41}_{\Lambda_b}\text{Ca}$
$1s_{1/2}$	-20.0	-19.5	-12.8	-16.3	-6.3	—	-9.9	-1.0	-23.0
$1p_{3/2}$	-12.0 (1p)	-12.3	-9.2	-13.2	-4.1	—	-6.7	—	-20.9
$1p_{1/2}$	-12.0 (1p)	-12.3	-9.1	-12.9	-3.8	—	-6.7	—	-20.9
$1d_{5/2}$		-4.7	-4.8	-9.9	—	—	-3.3	—	-18.4
$2s_{1/2}$		-3.5	-3.4	-9.3	—	—	-2.8	—	-17.4
$1d_{3/2}$		-4.6	-4.8	-9.4	—	—	-3.3	—	-18.4
	—	$^{49}_\Lambda\text{Ca}$	$^{49}_{\Lambda_c^+}\text{Ca}$	$^{49}_{\Sigma_c^0}\text{Ca}$	$^{49}_{\Sigma_c^+}\text{Ca}$	$^{49}_{\Sigma_c^{++}}\text{Ca}$	$^{49}_{\Xi_c^0}\text{Ca}$	$^{49}_{\Xi_c^+}\text{Ca}$	$^{49}_{\Lambda_b}\text{Ca}$
$1s_{1/2}$		-21.0	-14.3	—	-7.4	-5.0	-7.8	-5.1	-24.4
$1p_{3/2}$		-13.9	-10.6	-7.2	-5.1	-3.4	-4.1	-2.8	-22.2
$1p_{1/2}$		-13.8	-10.6	-7.0	-4.9	-3.2	-4.1	-2.8	-22.2
$1d_{5/2}$		-6.5	-6.5	-4.0	-2.3	—	-0.9	—	-19.5
$2s_{1/2}$		-5.4	-5.3	-4.9	—	—	-1.5	—	-18.8
$1d_{3/2}$		-6.4	-6.4	-3.6	-1.9	—	-1.0	—	-19.5
$1f_{7/2}$		—	-2.0	—	—	—	—	—	-16.8

Table 5: Single-particle energies (in MeV) for $^{91}_j\text{Zr}$ and $^{208}_j\text{Pb}$ ($j = \Lambda, \Lambda_c^+, \Sigma_c, \Xi_c, \Lambda_b$), calculated with the effective Pauli blocking and the $\Sigma_{c,b}N - \Lambda_{c,b}N$ channel coupling. Experimental data are taken from Ref. [46]. Spin-orbit splittings for the Λ hypernuclei are not well determined by the experiments.

	$^{89}_\Lambda\text{Yb}$ (Exp.)	$^{91}_\Lambda\text{Zr}$	$^{91}_{\Lambda_c^+}\text{Zr}$	$^{91}_{\Sigma_c^0}\text{Zr}$	$^{91}_{\Sigma_c^+}\text{Zr}$	$^{91}_{\Sigma_c^{++}}\text{Zr}$	$^{91}_{\Xi_c^0}\text{Zr}$	$^{91}_{\Xi_c^+}\text{Zr}$	$^{91}_{\Lambda_b}\text{Zr}$
$1s_{1/2}$	-22.5	-23.9	-10.8	—	-3.7	—	-9.3	—	-25.7
$1p_{3/2}$	-16.0 (1p)	-18.4	-8.7	-10.2	-2.3	—	-6.6	—	-24.2
$1p_{1/2}$	-16.0 (1p)	-18.4	-8.7	-10.1	-2.1	—	-6.7	—	-24.2
$1d_{5/2}$	-9.0 (1d)	-12.3	-5.8	-7.6	—	—	-4.0	—	-22.4
$2s_{1/2}$		-10.8	-3.9	-8.1	—	—	-3.9	—	-21.6
$1d_{3/2}$	-9.0 (1d)	-12.3	-5.8	-7.3	—	—	-4.0	—	-22.4
$1f_{7/2}$	-2.0 (1f)	-5.9	-2.4	-5.1	—	—	-1.3	—	-20.4
$2p_{3/2}$		-4.2	—	-5.0	—	—	-1.3	—	-19.5
$1f_{5/2}$	-2.0 (1f)	-5.8	-2.4	-4.7	—	—	-1.4	—	-20.4
$2p_{1/2}$		-4.1	—	-4.9	—	—	-1.3	—	-19.5
$1g_{9/2}$		—	—	-2.4	—	—	—	—	-18.1
	$^{208}_\Lambda\text{Pb}$ (Exp.)	$^{209}_\Lambda\text{Pb}$	$^{209}_{\Lambda_c^+}\text{Pb}$	$^{209}_{\Sigma_c^0}\text{Pb}$	$^{209}_{\Sigma_c^+}\text{Pb}$	$^{209}_{\Sigma_c^{++}}\text{Pb}$	$^{209}_{\Xi_c^0}\text{Pb}$	$^{209}_{\Xi_c^+}\text{Pb}$	$^{209}_{\Lambda_b}\text{Pb}$
$1s_{1/2}$	-27.0	-27.0	-5.2	-7.5	—	—	-6.7	—	-27.4
$1p_{3/2}$	-22.0 (1p)	-23.4	-4.1	-6.6	—	—	-5.4	—	-26.6
$1p_{1/2}$	-22.0 (1p)	-23.4	-4.0	-6.5	—	—	-5.5	—	-26.6
$1d_{5/2}$	-17.0 (1d)	-19.1	-2.4	-5.3	—	—	-3.9	—	-25.4
$2s_{1/2}$		-17.6	—	—	—	—	-3.3	—	-24.7
$1d_{3/2}$	-17.0 (1d)	-19.1	-2.4	-5.1	—	—	-4.0	—	-25.4
$1f_{7/2}$	-12.0 (1f)	-14.4	—	-3.8	—	—	-2.2	—	-24.1
$2p_{3/2}$		-12.4	—	—	—	—	-1.4	—	-23.2
$1f_{5/2}$	-12.0 (1f)	-14.3	—	-3.5	—	—	-2.3	—	-24.1
$2p_{1/2}$		-12.4	—	—	—	—	-1.5	—	-23.2
$1g_{9/2}$	-7.0 (1g)	-9.3	—	-2.1	—	—	—	—	-22.6
$1g_{7/2}$	-7.0 (1g)	-9.2	—	-1.8	—	—	—	—	-22.6
$1h_{11/2}$		-3.9	—	—	—	—	—	—	-21.0
$2d_{5/2}$		-7.0	—	—	—	—	—	—	-21.7
$2d_{3/2}$		-7.0	—	—	—	—	—	—	-21.7
$1h_{9/2}$		-3.8	—	—	—	—	—	—	-21.0
$3s_{1/2}$		-6.1	—	—	—	—	—	—	-21.3
$2f_{7/2}$		-1.7	—	—	—	—	—	—	-20.1
$3p_{3/2}$		-1.0	—	—	—	—	—	—	-19.6
$2f_{5/2}$		-1.7	—	—	—	—	—	—	-20.1
$3p_{1/2}$		-1.0	—	—	—	—	—	—	-19.6
$1i_{13/2}$		—	—	—	—	—	—	—	-19.3

center of the hypernucleus. However, always a proper level with lower energy than those of the $1p_{1/2}$, $1p_{3/2}$ and $2s_{1/2}$ states could not be found. In such case, the single-particle energy level became equal or higher than that of the $2s_{1/2}$ state, which is also above the levels of the $1p_{1/2}$ and $1p_{3/2}$ states. In the search procedure, we always checked also the core nucleon single-particle energy levels to be in correct order. However, whenever we get the lower single-particle energy level for the $1s_{1/2}$ state than those for the $1p_{1/2}$, $1p_{3/2}$ and $2s_{1/2}$ states, the core neutron $1s_{1/2}$ energy level jumped to become equal or larger than that of the $2s_{1/2}$, and we discarded the results in such cases. In this manner, the $1s_{1/2}$ state in $^{17}_{\Sigma_c^0}$ O, $^{49}_{\Sigma_c^0}$ Ca and $^{91}_{\Sigma_c^0}$ Zr could not be found. This is probably because the phenomenologically introduced channel coupling effect for the Σ_c is too strong, particularly near the central region of the hypernucleus, due to the correlation with the core nucleons by the self-consistent procedure. In fact, when we use the same strength for the Σ_c as that for the Λ , Λ_c^+ and Λ_b , i.e., $\tilde{\lambda}_{\Sigma_c} = \lambda_{\Lambda_c^+}$, we get the correct order of single-particle energies together with those for the core nucleons. Furthermore, when $\tilde{\lambda}_{\Sigma} = \tilde{\lambda}_{\Sigma_c}$ was applied for the $\Sigma^{-,0,+}$ strange hypernuclei [9], the correct single-particle energy levels were obtained. The main difference in the calculation for the Σ_c hypernuclei from that for the Σ hypernuclei is the bare (effective) mass, where mass of the Σ_c is much larger, and the wave function (if obtained) for the $1s_{1/2}$ is expected to be localized much more in the central region of each Σ_c hypernucleus when the isospin dependent and Coulomb forces are neglected. This may also be a consequence of a subtle interplay between the isospin dependent force for the Σ_c^0 (the isospin third component is -1), and baryonic density in the central region. Thus, we think the results for the Σ_c hypernuclei may be an indication of the artifact how the $\Sigma_c N - \Lambda_c N$ channel coupling is introduced. In a limiting case, one may disregard the results for them, although actually the $\Sigma_c N - \Lambda_c N$ channel coupling effect is expected to be smaller than that for the $\Sigma N - \Lambda N$, when the same strength for the effect is applied, and that is the case in the present study.

Next, in order to understand the obtained single-particle energies better, we first show in Fig. 3 the total baryon density distributions for the $1s_{1/2}$ configuration in $^{41}_{\Lambda, \Lambda_c^+, \Lambda_b}$ Ca. Note that because of the self-consistency, the total baryon density distributions are dependent on the configurations of the embedded particle. The total baryon density distributions are quite similar for the Λ , Λ_c^+ and Λ_b hypernuclei multiplet which have the same baryon number A , since the effect of the Λ , Λ_c^+ and Λ_b is, $\simeq M_{\Lambda, \Lambda_c, \Lambda_b} / [(A-1)M_N + M_{\Lambda, \Lambda_c, \Lambda_b}]$, for each hypernucleus. Nevertheless, it is important to note that for the Λ_b hypernuclei total baryon density near the center is slightly higher than the corresponding Λ and Λ_c^+ hypernuclei. This is because the Λ_b is heavy and localized nearer the center, and contributes to the total baryon density there. The baryon (probability) density distributions for the Λ , Λ_c^+ and Λ_b in the corresponding hypernuclei will be shown later. One can expect similar features for the other heavy baryon hypernuclei as for the total baryon density distributions, since the effect of the embedded heavy baryon is small again, and is, $\simeq M_C / [(A-1)M_N + M_C]$.

Next, in Figs. 4-7 we show the potential strengths (scalar, vector, Coulomb, Pauli blocking plus channel coupling) for the $1s_{1/2}$ state those found in $^{41}_j$ Ca and $^{209}_j$ Pb ($j = \Lambda, \Lambda_c^+, \Lambda_b, \Sigma_c^{0,+}, \Xi_c^0$). “Pauli” stands for the effective, repulsive, potential representing the Pauli blocking at the quark level plus the $\Sigma_{c,b}N - \Lambda_{c,b}N$ channel coupling for the Λ and $\Lambda_{c,b}$ hypernuclei introduced in Eq. (46). “Pa+CC.” stands for the effective Pauli blocking plus channel coupling potential for the $\Sigma_c^{0,+}$ hypernuclei. Recall that the effects are different for the Λ_c^+ and Σ_c as they are also true for the Λ and Σ . For the charged heavy baryons, the Coulomb potentials are also shown. As in the limit of nuclear matter in Section 2.2, the scalar and vector potentials for the heavy

baryons are also quite similar to the strange hyperons with the same light quark numbers in the corresponding hypernuclei. This feature also holds between the Σ_c and Σ in the corresponding hypernuclei, except for contributions due to the differences in charges, where the Coulomb force affects the baryon density distributions and then the vector and scalar potentials are also slightly modified. Thus, as far as the total baryon density distributions and the scalar and vector potentials are concerned, among/between the members within each multiplet, $(\Lambda, \Lambda_c^+, \Lambda_b)$, (Σ, Σ_c) and (Ξ, Ξ_c) hypernuclei, they show quite similar features. However, in realistic nuclei, the Coulomb force plays a crucial role as mentioned before, and the obtained single-particle energies show very different features within each hypernuclei multiplet. Of course, the mass differences within the multiplet is also the dominant source for the differences in the obtained single-particle energies.

Next, in Figs. 8 and 9 we show the probability density distributions for the heavy baryons for the $1s_{1/2}$ state, in $^{40}_j\text{Ca}$ and $^{209}_j\text{Pb}$ ($j = \Lambda, \Lambda_c^+, \Lambda_b, \Sigma_c^{0,+}, \Xi_c^0$). For the Λ, Λ_c^+ and Λ_b hypernuclei shown in Fig. 8, it is pronounced that the wave functions obtained (probability density distributions) are very different. The Λ_c^+ baryon density distribution in $^{209}_{\Lambda_c^+}\text{Pb}$ is much more pushed away from the center than that for the Λ in ^{209}Pb due to the Coulomb force. On the contrary, the Λ_b baryon density distributions in Λ_b hypernuclei are much larger near the center than those for the Λ in the corresponding Λ hypernuclei due to its heavy mass.

It is interesting to compare the Σ_c^0 and Ξ_c^0 probability density distributions shown in Fig. 9. Due to the effects of the Pauli blocking and the channel coupling, the probability density distributions for the Σ_c^0 are pushed away than those for the Ξ_c^0 in both $^{41}_{\Sigma_c^0}\text{Ca}$ and $^{209}_{\Sigma_c^0}\text{Pb}$. In particular, the Σ_c^0 density distributions in ^{209}Pb are really pushed away from the central region, and thus nearly losing the character of a typical $1s_{1/2}$ state wave function, i.e., the probability density distributions near the center of the nucleus become very small compared to those correspond to the usual $1s_{1/2}$ state. Thus, one can imagine that it is very difficult for the $\Sigma_c^+ 1s_{1/2}$ state to exist in $^{209}_{\Sigma_c^+}\text{Pb}$, since the additional Coulomb repulsion works to push further the Σ_c^+ away from the central region. Thus, the probability density there may be nearly zero, and this may be a reason why no convergent solution is obtained for the $1s_{1/2}$ state wave function. On the contrary, it is rather surprising that the Ξ_c^0 probability density distributions are higher and localized in the central region than those for the $\Sigma_c^{0,+}$, although one can naively expect that they have an opposite characteristic, because of the smaller scalar attractive potential for the Ξ_c^0 . Thus, in the present calculation the effects of the Pauli blocking, and particularly the channel coupling, play a crucial role for these different features. Then, we must be careful to draw any solid conclusions from the Σ_c^0 and Σ_c^+ probability density distributions.

Finally, we show in Table 6 the calculated binding energy per baryon, $-E/A$, r.m.s charge radius, r_{ch} , and r.m.s radii of the heavy baryon, neutron and proton distributions, r_C , r_n and r_p , respectively. The results listed in Table 6 are calculated with the $1s_{1/2}$ heavy baryon configuration for all cases. At a first glance, it is very clear that the r.m.s radius for the Λ_b is very small compared to those for other baryons within the same baryon number hypernuclei as one would expect, due to heavy mass. The radii, r_{ch} , r_n and r_p , are more or less similar for all heavy baryon hypernuclei and Λ hypernuclei within the same baryon number multiplet, reflecting the fact that the effect of the embedded baryon on these quantities are of order, $\simeq M_{C,\Lambda}/[(A-1)M_N + M_{C,\Lambda}]$. As for the binding energy per baryon, the energy of Λ_b hypernuclei is usually the largest among the same baryon number hypernuclei. One of the largest contributions for this is the single-particle energy of the $1s_{1/2}$ state, even after dividing

Table 6: Binding energy per baryon, $-E/A$ (in MeV), r.m.s charge radius, r_{ch} , and r.m.s radii of the Λ and heavy baryons, r_j , neutron, r_n , and proton, r_p (in fm) for $^{17}_j\text{O}$, $^{41}_j\text{Ca}$, $^{49}_j\text{Ca}$, $^{91}_j\text{Zr}$ and $^{209}_j\text{Pb}$ ($j = \Lambda, \Lambda_c^+, \Sigma_c, \Xi_c, \Lambda_b$). The configurations of the Λ and heavy baryon j , are $1s_{1/2}$ for all hypernuclei. Results for the Λ hypernuclei are taken from Ref. [9].

hypernuclei	$-E/A$	r_{ch}	r_j	r_n	r_p
$^{17}_\Lambda\text{O}$	6.37	2.84	2.49	2.59	2.72
$^{17}_{\Lambda_c^+}\text{O}$	6.42	2.85	2.19	2.58	2.73
$^{17}_{\Sigma_c^+}\text{O}$	6.10	2.83	2.57	2.60	2.71
$^{17}_{\Xi_c^0}\text{O}$	6.01	2.81	2.34	2.61	2.69
$^{17}_{\Xi_c^+}\text{O}$	5.84	2.81	2.70	2.61	2.69
$^{17}_{\Lambda_b}\text{O}$	6.69	2.87	1.81	2.57	2.75
$^{41}_\Lambda\text{Ca}$	7.58	3.51	2.81	3.31	3.42
$^{41}_{\Lambda_c^+}\text{Ca}$	7.58	3.51	2.66	3.31	3.42
$^{41}_{\Sigma_c^0}\text{Ca}$	7.54	3.51	2.79	3.31	3.42
$^{41}_{\Sigma_c^+}\text{Ca}$	7.42	3.50	3.21	3.31	3.41
$^{41}_{\Xi_c^0}\text{Ca}$	7.43	3.49	2.76	3.32	3.40
$^{41}_{\Xi_c^+}\text{Ca}$	7.32	3.49	3.11	3.32	3.39
$^{41}_{\Lambda_b}\text{Ca}$	7.72	3.53	2.22	3.30	3.43
$^{49}_\Lambda\text{Ca}$	7.58	3.54	2.84	3.63	3.45
$^{49}_{\Lambda_c^+}\text{Ca}$	7.54	3.54	2.67	3.63	3.45
$^{49}_{\Sigma_c^0}\text{Ca}$	7.39	3.54	3.17	3.64	3.44
$^{49}_{\Sigma_c^+}\text{Ca}$	6.29	3.57	3.62	3.71	3.47
$^{49}_{\Xi_c^0}\text{Ca}$	7.34	3.53	2.57	3.65	3.43
$^{49}_{\Xi_c^+}\text{Ca}$	7.32	3.53	3.19	3.65	3.43
$^{49}_{\Lambda_b}\text{Ca}$	7.64	3.56	2.16	3.63	3.46
$^{91}_\Lambda\text{Zr}$	7.95	4.29	3.25	4.29	4.21
$^{91}_{\Lambda_c^+}\text{Zr}$	7.85	4.29	3.34	4.30	4.21
$^{91}_{\Sigma_c^+}\text{Zr}$	7.77	4.29	4.03	4.30	4.21
$^{91}_{\Xi_c^0}\text{Zr}$	7.78	4.28	3.01	4.30	4.20
$^{91}_{\Lambda_b}\text{Zr}$	7.93	4.30	2.63	4.29	4.22
$^{209}_\Lambda\text{Pb}$	7.35	5.49	3.99	5.67	5.43
$^{209}_{\Lambda_c^+}\text{Pb}$	7.26	5.49	4.74	5.68	5.43
$^{209}_{\Sigma_c^0}\text{Pb}$	6.95	5.51	4.88	5.70	5.45
$^{209}_{\Xi_c^0}\text{Pb}$	7.24	5.49	4.44	5.68	5.43
$^{209}_{\Lambda_b}\text{Pb}$	7.48	5.49	3.45	5.66	5.43

by the total baryon number. (See Eq. (43).)

5 Summary and discussion

In summary, we have studied systematically the possibilities of the low-lying heavy baryon hypernuclei, Λ_c^+ , Σ_c , Ξ_c and Λ_b hypernuclei in the QMC model, adopting the same methods as those applied for the study of strange hypernuclei [9]. The spin-orbit potentials for the heavy baryon hypernuclei are negligible for the single-particle energies, because of their heavy masses. Our results suggest that the formation of Λ_c^+ , Ξ_c^0 and Λ_b hypernuclei is expected quite likely, while that of the Σ_c^{++} and Ξ_c^+ is unlikely. For the Σ_c^0 and Σ_c^+ hypernuclei, although there may be some possibilities to be formed, it is difficult to draw a solid conclusion in view of the ambiguities and approximations made in the calculations.

For the Λ , Λ_c^+ and Λ_b hypernuclei, although the total baryon density distributions and the scalar and vector potentials are quite similar, the wave functions obtained, e.g., for the $1s_{1/2}$ state, are very different. The Λ_c^+ baryon density distribution in $^{209}_{\Lambda_c^+}\text{Pb}$ is much more pushed away from the center than that for the Λ in $^{209}_{\Lambda}\text{Pb}$ due to the Coulomb force. On the contrary, the Λ_b baryon density distributions in Λ_b hypernuclei are much larger near the origin than those for the Λ in the corresponding Λ hypernuclei due to its heavy mass.

For the Σ_c and Ξ_c hypernuclei, the Coulomb force is crucial in the possibility to form the hypernuclei, in particular for the $\Sigma_c^{+,++}$ hypernuclei. The results for the Σ_c hypernuclei imply that the phenomenologically introduced channel coupling effects are very crucial, although the effects may be overestimated using the same strength as that for the Σ hypernuclei. Thus, we need to investigate further how such effects can be included consistently with the underlying quark structure. In this sense, some of the results for the Σ_c hypernuclei need to be taken with a caution.

Although there can be numerous speculations on the implications of the present results we would like to emphasize that our calculations indicate that the Λ_c^+ , Ξ_c^0 , and Λ_b hypernuclei would exist in realistic experimental conditions, but there may be lesser possibilities for the Σ_c^0 and Σ_c^+ hypernuclei. Furthermore, it is very unlikely for the Σ_c^{++} and Ξ_c^+ hypernuclei will be formed. Experiments at facilities like JHF would provide quantitative input to gain a better understanding of the interactions of heavy baryons with nuclear matter. Experiments at colliders such as RHIC, LHC and Fermilab could provide additional data to establish the formation and decay of such heavy baryon hypernuclei. A combination of these data and a careful analysis, with the present calculations being considered as a first step, would give a valuable information about the physical implications for the presence of heavy quarks in finite or dense nuclear matter. Eventually these results can have important implications for studies in astrophysics of neutron stars and nuclear matter at very high densities.

As for the other aspects of interests for the properties of heavy baryons in nuclear medium, additional studies are needed to investigate the semi-leptonic weak decay of Λ_c^+ , Σ_c , Ξ_c and Λ_b hyperons in nuclear medium. The role of Pauli blocking and density in influencing the decay rates as compared to the free heavy baryons would be highly useful. Such studies can have an impact on the hadronization of the quark-gluon plasma and the transport of hadrons in nuclear matter of high density. Will the high density lead to a slower decay and that a higher probability to survive its passage through the material ? At present the study of the presence of heavy baryons in finite nuclei is in its infancy. Careful investigations, both theoretical and

experimental, would lead to a much better understanding of the role of heavy quarks and/or heavy baryons in finite nuclei.

Acknowledgment

The authors would like to thank Prof. A.W. Thomas for the hospitality at CSSM, Adelaide, where this work was initiated. KT acknowledges support and warm hospitality at University of Alberta, where main part of the calculation was completed. KT is supported by the Forschungszentrum-Jülich, contract No. 41445282 (COSY-058). The work of FK is supported by NSERC.

References

- [1] K. Tsushima, F.C. Khanna, Phys. Lett. B 552 (2003) 138.
- [2] P.A.M. Guichon, Phys. Lett. B 200 (1989) 235.
- [3] A.A. Tyapkin, Sov. J. Nucl. Phys. 22 (1976) 89.
- [4] C.B. Dover and S.H. Kahana, Phys. Rev. Lett. 39 (1977) 1506.
- [5] B.F. Gibson, C.B. Dover, G. Bhamati, and D.R. Lehman, Phys. Rev. C 27 (1982) 2085.
- [6] H. Bando, and M. Bando, Phys. Lett. B 109 (1982) 164;
H. Bando, and S. Nagata, Prog. Theor. Phys. 69 (1983) 557.
- [7] T. Bressani, F. Iazzi, Nuovo. Cim. 102 A (1989) 597; S.A. Buyatov, V.V. Lyukov, N.I. Strakov and V.A. Tsarev, Nuovo. Cim. 104 A (1991) 1361.
- [8] K. Tsushima, F.C. Khanna, Phys. Rev. C 67 (2003) 015211;
nucl-th/0212100, to be published in the YITP proceedings “Chiral Restoration in Nuclear Physics”, Prog. Theor. Phys. Suppl. 149 (2003).
- [9] K. Tsushima, K. Saito, J. Haidenbauer, A.W. Thomas, Nucl. Phys. A 630 (1998) 691;
K. Tsushima, K. Saito, A.W. Thomas, Phys. Lett. B 411 (1997) 9; (E) *ibid.* B 421 (1998) 413.
- [10] For example, the Proceedings of Joint CSSM/JHF/NITP Workshop on Physics at the Japan Hadron Facility, Adelaide, Australia, 14-21 Mar 2002, Eds. V. Guzey, A. Kizilersü, T. Nagae, & A.W. Thomas, World Scientific, 2002.
- [11] P.A.M. Guichon, K. Saito, E.N. Rodionov, A.W. Thomas Nucl. Phys. A 601 (1996) 349;
P.A.M. Guichon, K. Saito, A.W. Thomas, nucl-th/9602022, Austral. J. Phys. 50 (1997) 115.
- [12] K. Saito, K. Tsushima, A.W. Thomas, Nucl. Phys. A 609 (1996) 339.
- [13] K. Saito and A.W. Thomas, Phys. Lett. B 327 (1994) 9;
K. Saito and A.W. Thomas, Phys. Rev. C 51 (1995) 2757;
K. Saito and A.W. Thomas, Phys. Rev. C 52 (1995) 2789;

- [14] K. Tsushima, K. Saito, A.W. Thomas, Phys. Lett. B 465 (1999) 27;
 D.H. Lu, K. Tsushima, A.W. Thomas, A.G. Williams, K. Saito, Phys. Lett. B 417 (1998) 217; Phys. Lett. B 441 (1998) 27;
 Nucl. Phys. A 634 (1998) 443; Phys. Rev. C 60 (1999) 068201;
 F.M. Steffens, K. Tsushima, A.W. Thomas, K. Saito, Phys. Lett. B 447 (1999) 233;
 K. Saito, K. Tsushima, A.W. Thomas, Phys. Lett. B 460 (1999) 17; Phys. Lett. B 465 (1999) 27;
 K. Tsushima, K. Saito, A.W. Thomas, Phys. Lett. B 465 (1999) 36;
 K. Tsushima, in the proceedings, *ISHEP 98*, Dubna, Russia, 17-22 Aug 1998, nucl-th/9811063; Nucl. Phys. A 670 (2000) 198c;
 K. Tsushima, A. Sibirtsev, K. Saito, A.W. Thomas, D.H. Lu, Nucl. Phys. A 680 (2001) 280c;
 K. Saito, K. Tsushima, Prog. Theor. Phys. 105 (2001) 373;
 W. Melnitchouk, K. Tsushima, A.W. Thomas, Eur. Phys. J. A14 (2002) 105;
 K. Tsushima, hep-ph/0206069, in the proceedings of Joint CSSM/JHF/NITP Workshop on Physics at the Japan Hadron Facility, Adelaide, Australia, 14-21 Mar 2002, p. 303, Eds. V. Guzey, A. Kizilersü, T. Nagae, & A.W. Thomas, World Scientific, 2002.
- [15] K. Tsushima D.H. Lu, A.W. Thomas, K. Saito, Phys. Lett. B 443 (1998) 26.
- [16] K. Tsushima, D.H. Lu, A.W. Thomas, K. Saito, R.H. Landau, Phys. Rev. C 59 (1999) 2824.
- [17] For recent applications of QMC, e.g., K. Tsushima et al., nucl-th/0301078, to be published in the Proceedings of the Joint JLab-UGA Workshop on “Modern Sub-Nuclear Physics and JLab Experiments”, Sep. 13, 2002, Athens Georgia, USA.
- [18] A. Sibirtsev, K. Tsushima, K. Saito, A.W. Thomas, Phys. Lett. B 484 (2000) 23.
- [19] A. Sibirtsev, K. Tsushima, A.W. Thomas, Eur. Phys. J. A 6 (1999) 351.
- [20] K. Tsushima, K. Saito, A.W. Thomas, S.V. Wright, Phys. Lett. B 429 (1998) 239; (E) *ibid.* B 436 (1998) 453;
 K. Tsushima, A. Sibirtsev, A.W. Thomas, Phys. Rev. C 62 (2000) 064904; J. Phys. G 27 (2001) 349.
- [21] P.G. Blunden and G.A. Miller, Phys. Rev. C 54 (1996) 359.
- [22] X. Jin and B.K. Jennings, Phys. Lett. B 374 (1996) 13;
 X. Jin and B.K. Jennings, Phys. Rev. C 54 (1996) 1427; *ibid* Phys. Rev. C 55 (1997) 1567.
- [23] S. Fleck et al., Nucl. Phys. A 510 (1990) 731;
 V.K. Mishra et al., Phys. Rev. C 46 (1992) 1143;
 M.K. Banerjee, Phys. Rev. C 45 (1992) 1359;
 E. Naar and M.C. Birse, J. Phys. G 19 (1993) 555.
- [24] A. Hayashigaki, Prog. Theor. Phys. 101 (1999) 923.
- [25] F. Klingl, S. Kim, S.H. Lee, P. Morath, W. Weise, Phys. Rev. Lett. 82 (1999) 3396.

- [26] A. Hayashigaki, Phys. Lett. B 487 (2000) 96.
- [27] S. Dietrich et al., Phys. Lett. B 500 (2001) 47;
S. Malov et al. (JLab Hall A Collaboration), Phys. Rev. C 62 (2000) 057302; R.D. Ransome, Nucl. Phys. A 699 (2002) 360c.
- [28] S. Strauch et al., nucl-ex/0211022.
- [29] K. Saito, K. Tsushima, A.W. Thomas, Phys. Rev. C 55 (1997) 2637; Phys. Rev. C 56 (1997) 566.
- [30] G. Krein, A.W. Thomas, K. Tsushima, Nucl. Phys. A 650, (1999) 313.
- [31] K. Saito, and K. Tsushima, Prog. Theor. Phys. 105 (2001) 373.
- [32] R.I. Sawafta for the E887 and E905 Collaborations, Nucl. Phys. A 639, (1998) 103c;
S. Bart et. al., Phys. Rev. Lett. 83 (1999) 5238.
- [33] J.K. Ahn et al., Phys. Rev. Lett. 87 (2001) 132504;
H. Takahashi et al., Phys. Rev. Lett. 87 (2001) 212502.
- [34] J.D. Walecka, Ann. Phys. (N.Y.) 83 (1974) 491;
B.D. Serot and J.D. Walecka, Adv. Nucl. Phys. 16 (1986) 1.
- [35] R.J. Furnstahl and B.D. Serot, Nucl. Phys. A 468 (1987) 539.
- [36] J. Cohen, Phys. Rev. C 48 (1993) 1346.
- [37] J. Cohen and R.J. Furnstahl, Phys. Rev. C 35 (1987) 2231.
- [38] Particle Data Group, Phys. Rev. D 66 (2002) 010001.
- [39] J. Mareš and J. Žofka, Z. Phys. A 333 (1989) 209.
- [40] M. Rufa, H. Stöcker, P-G Reinhard, J. Maruhn and W. Greiner, J. Phys. G13 (1987) L143.
- [41] E.D. Cooper, B.K. Jennings, J. Mareš, Nucl. Phys. A 580 (1994) 419;
J. Mareš and B.K. Jennings, Phys. Rev. C 49 (1994) 2472;
J. Mareš, B.K. Jennings and E.D. Cooper, Prog. Theor. Phys. Supp. 117 (1994) 415;
J. Mareš and B.K. Jennings, Nucl. Phys. A 585 (1995) 347c;
J. Mareš, E. Friedman, A. Gal, B.K. Jennings, Nucl. Phys. A 594 (1995) 311.
- [42] B.K. Jennings, Phys. Lett. B 246 (1990) 325;
M. Chiapparini, A.O. Gattone, B.K. Jennings, Nucl. Phys. A 529 (1991) 589.
- [43] J. Cohen and H.J. Weber, Phys. Rev. C 44 (1991) 1181.
- [44] C.B. Dover and A. Gal, Prog. Part. Nucl. Phys. 12 (1985) 171.
- [45] R.E. Chrien A478 (1988) 705c.
- [46] S. Ajimura et al., Nucl. Phys. A 585 (1995) 173c.

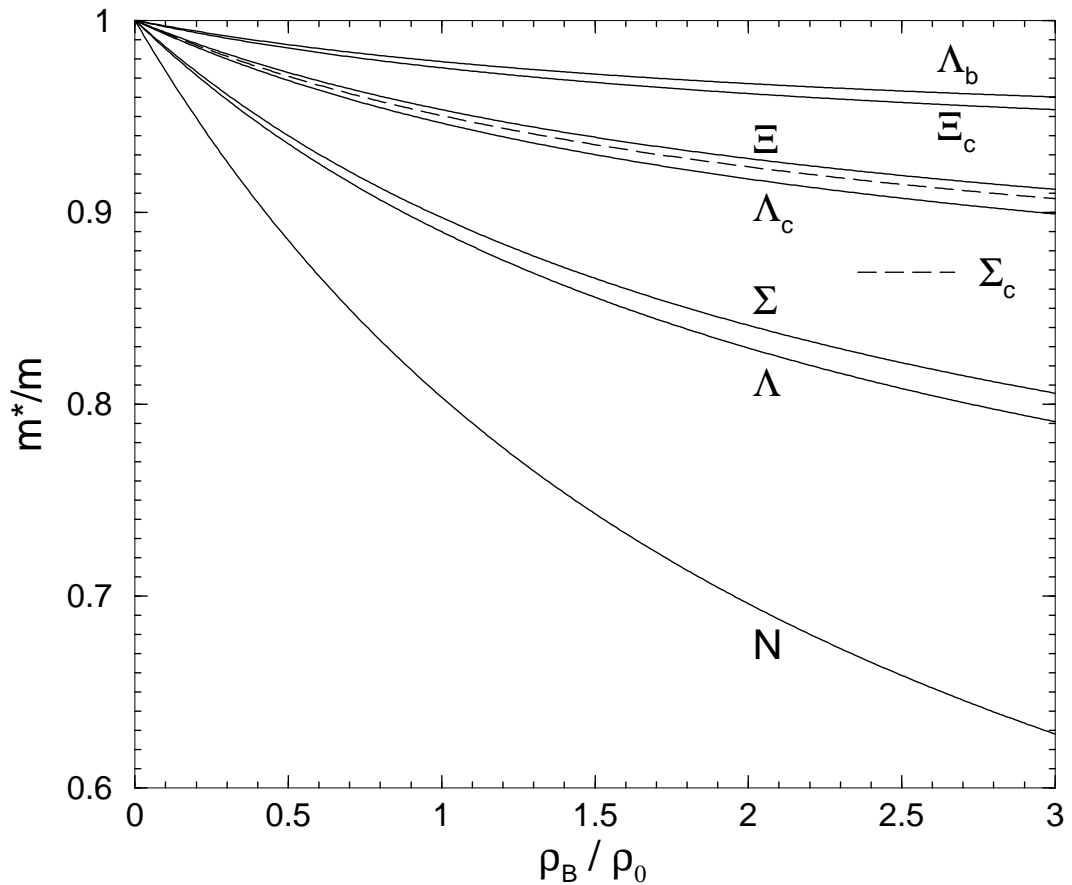


Figure 1: Effective mass ratios for baryons in nuclear matter. m^* and m stand for the masses in free space and in nuclear matter, respectively, where $\rho_0 = 0.15 \text{ fm}^{-3}$.

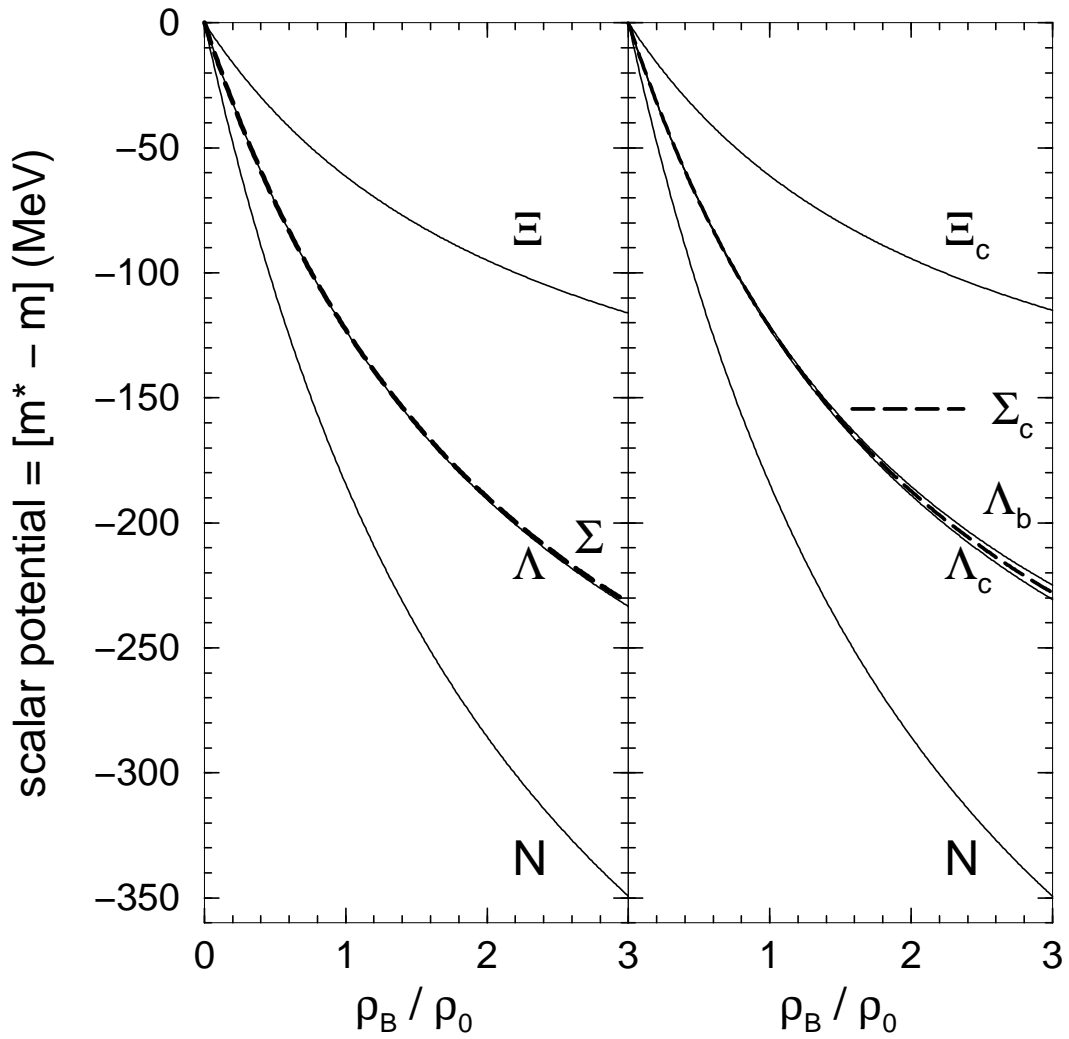


Figure 2: Scalar potentials for hyperons, low-lying charmed and bottom baryons in nuclear matter. See also caption of Fig. 1.

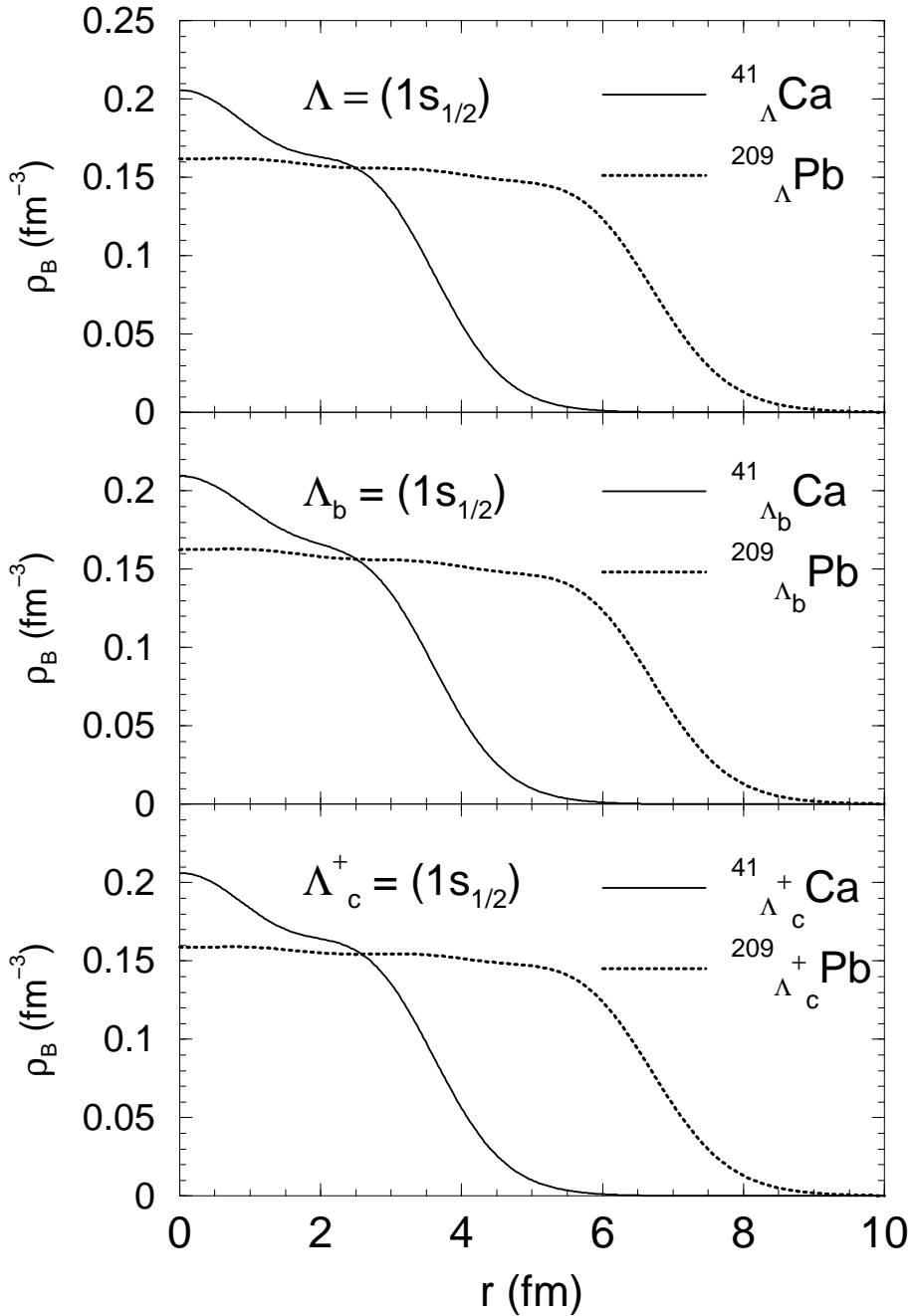


Figure 3: Total baryon density distributions in ${}^4{}_j\text{Ca}$ and ${}^{209}{}_j\text{Pb}$ ($j = \Lambda, \Lambda_c^+, \Lambda_b$) for the $1s_{1/2}$ state for the Λ, Λ_c^+ and Λ_b .

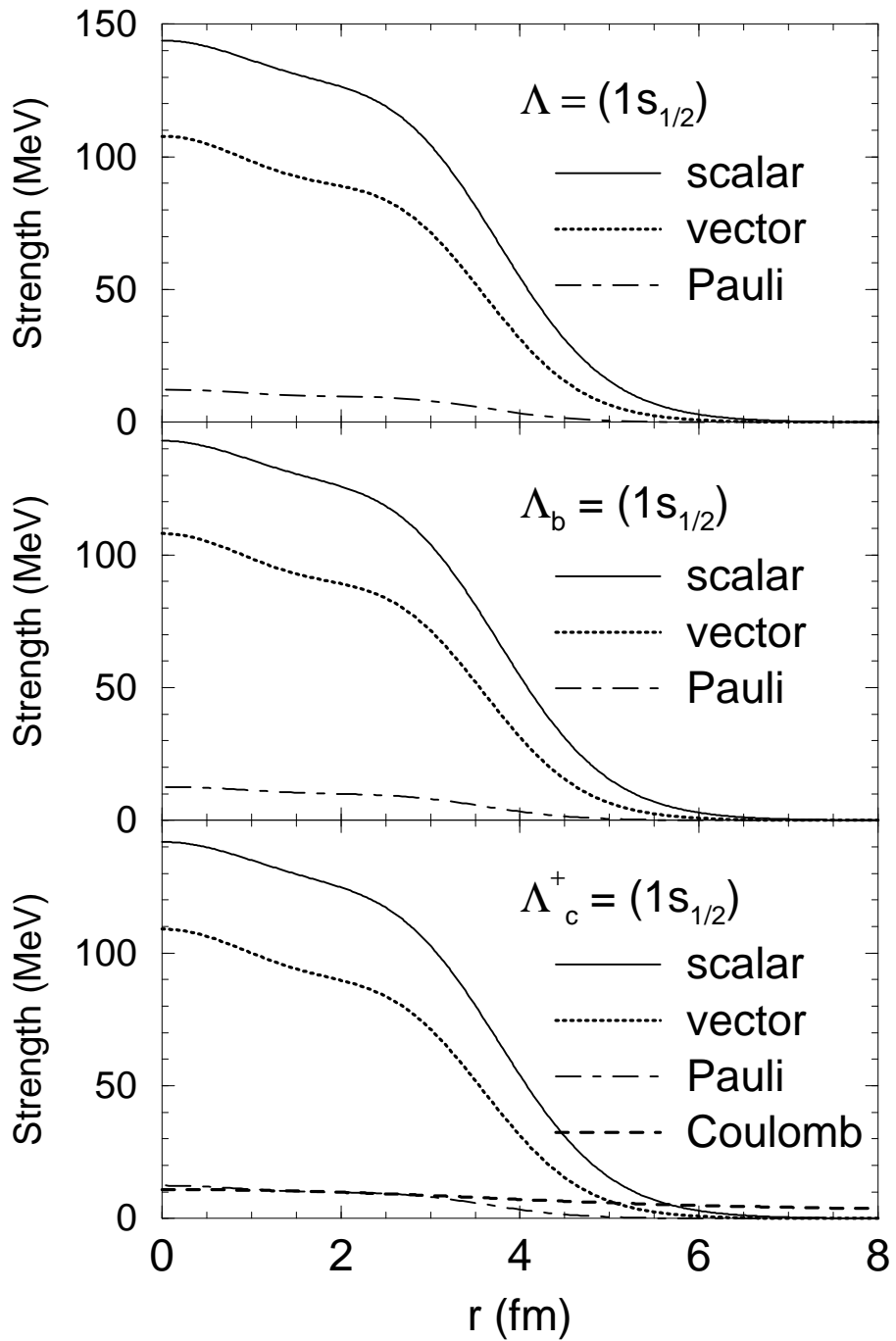


Figure 4: Potential strengths for the Λ , Λ_c^+ and Λ_b in ^{41}Ca ($j = \Lambda, \Lambda_c^+, \Lambda_b$) for the $1s_{1/2}$ state. (Scalar potential strength is multiplied by a factor, -1.) “Pauli” stands for the effective, repulsive, potential representing the Pauli blocking (plus the $\Sigma_{c,b}N - \Lambda_{c,b}N$ channel coupling), introduced at the hadronic level phenomenologically [9]. See also Eq. (46).

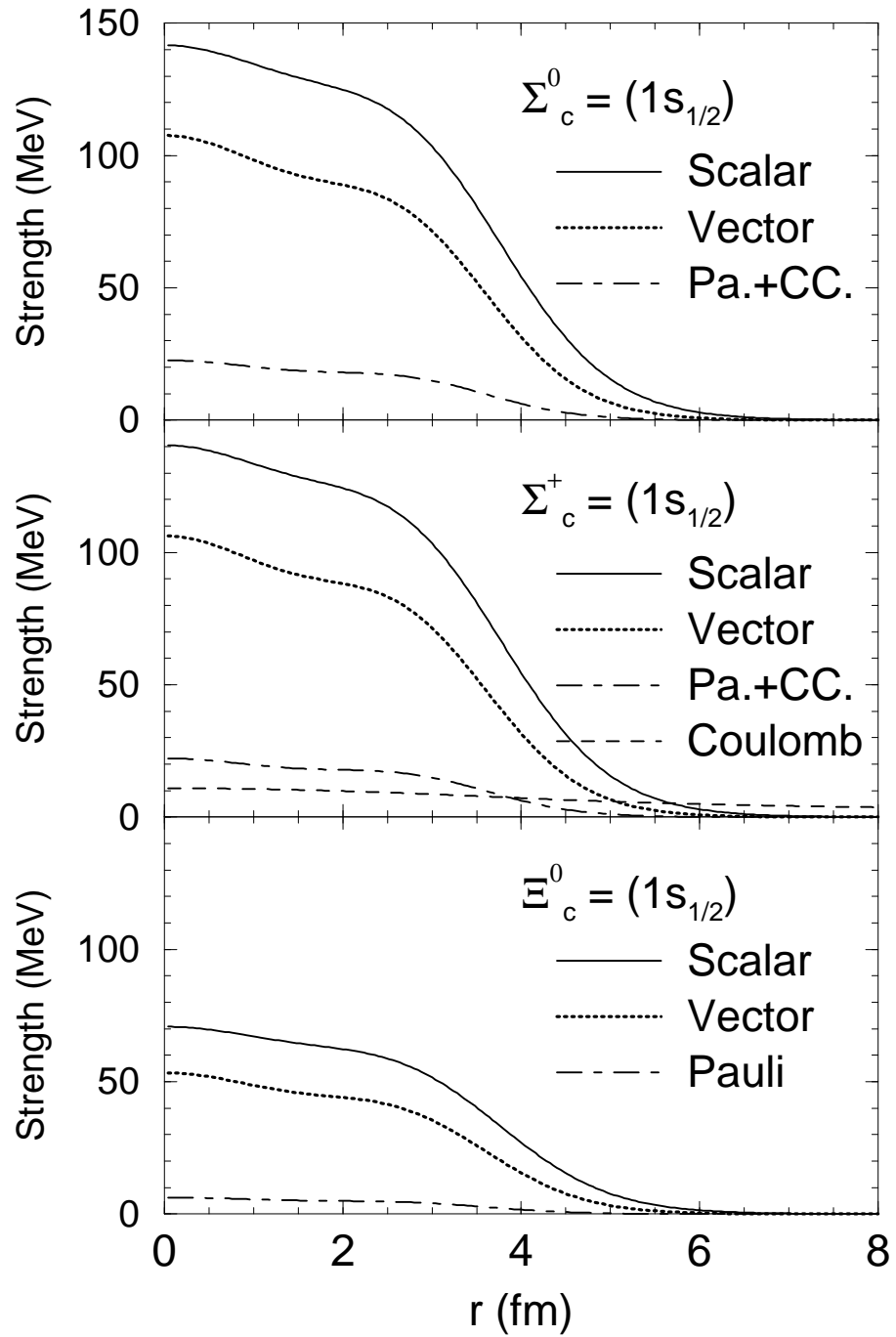


Figure 5: Potential strengths for the $\Sigma_c^{0,+}$ and Ξ_c^0 in $^{41}_j\text{Ca}$ ($j = \Sigma_c^{0,+}, \Xi_c^0$) for the $1s_{1/2}$ state. “Pa.+CC.” stands for potential for the effective Pauli blocking plus the channel coupling for the Σ_c . See also caption of Fig. 4.

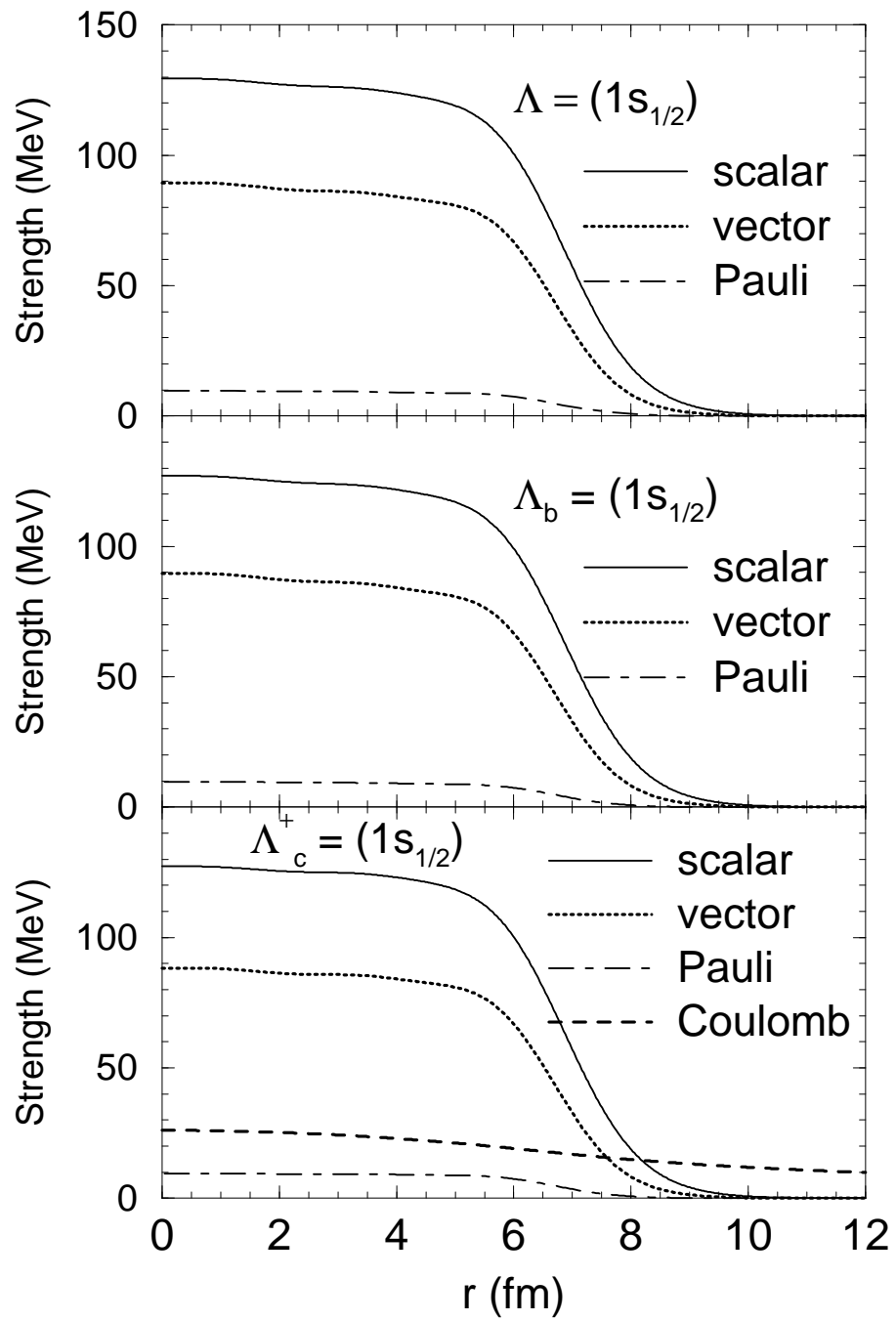


Figure 6: Potential strengths for the Λ , Λ_c^+ and Λ_b in ^{209}Pb ($j = \Lambda, \Lambda_c^+, \Lambda_b$) for the $1s_{1/2}$ state. See also caption of Fig. 4.

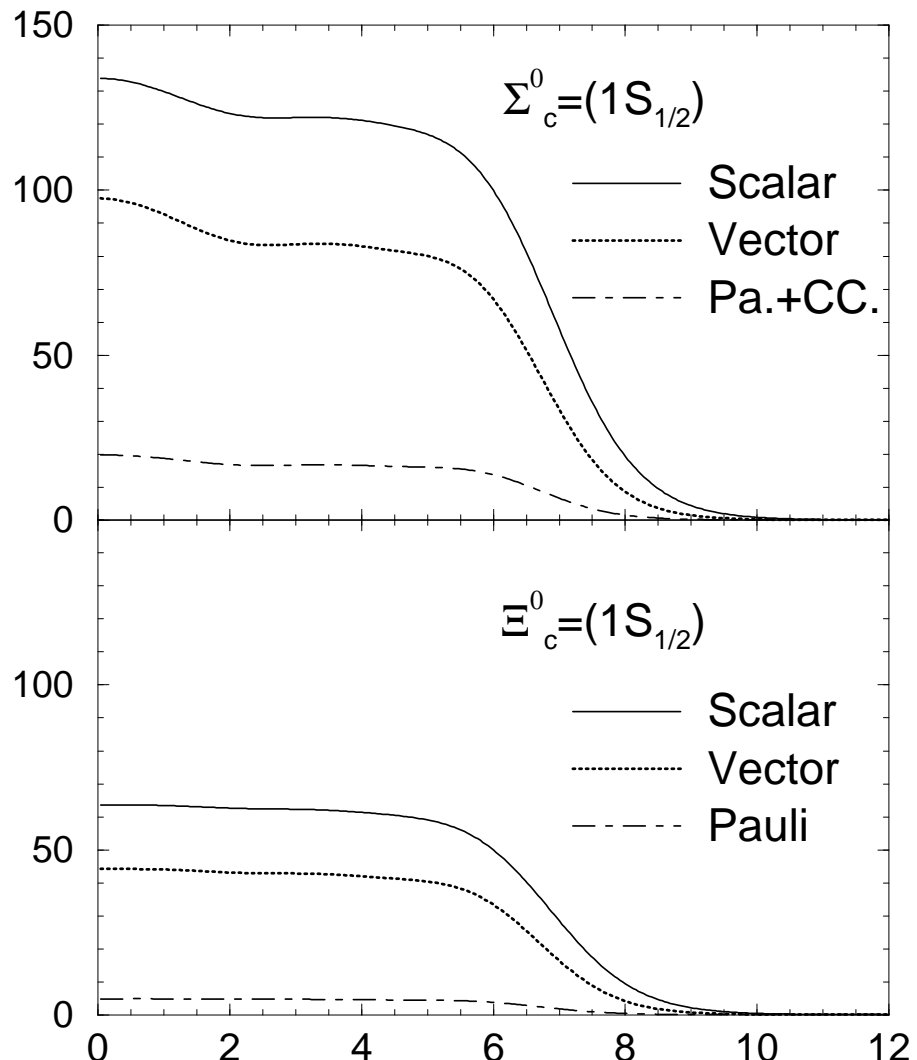


Figure 7: Potential strengths for the Σ_c^0 and Ξ_c^0 in $^{209}_{j}\text{Pb}$ ($j = \Sigma_c^0, \Xi_c^0$) for the $1s_{1/2}$ state. See also caption of Fig. 5.

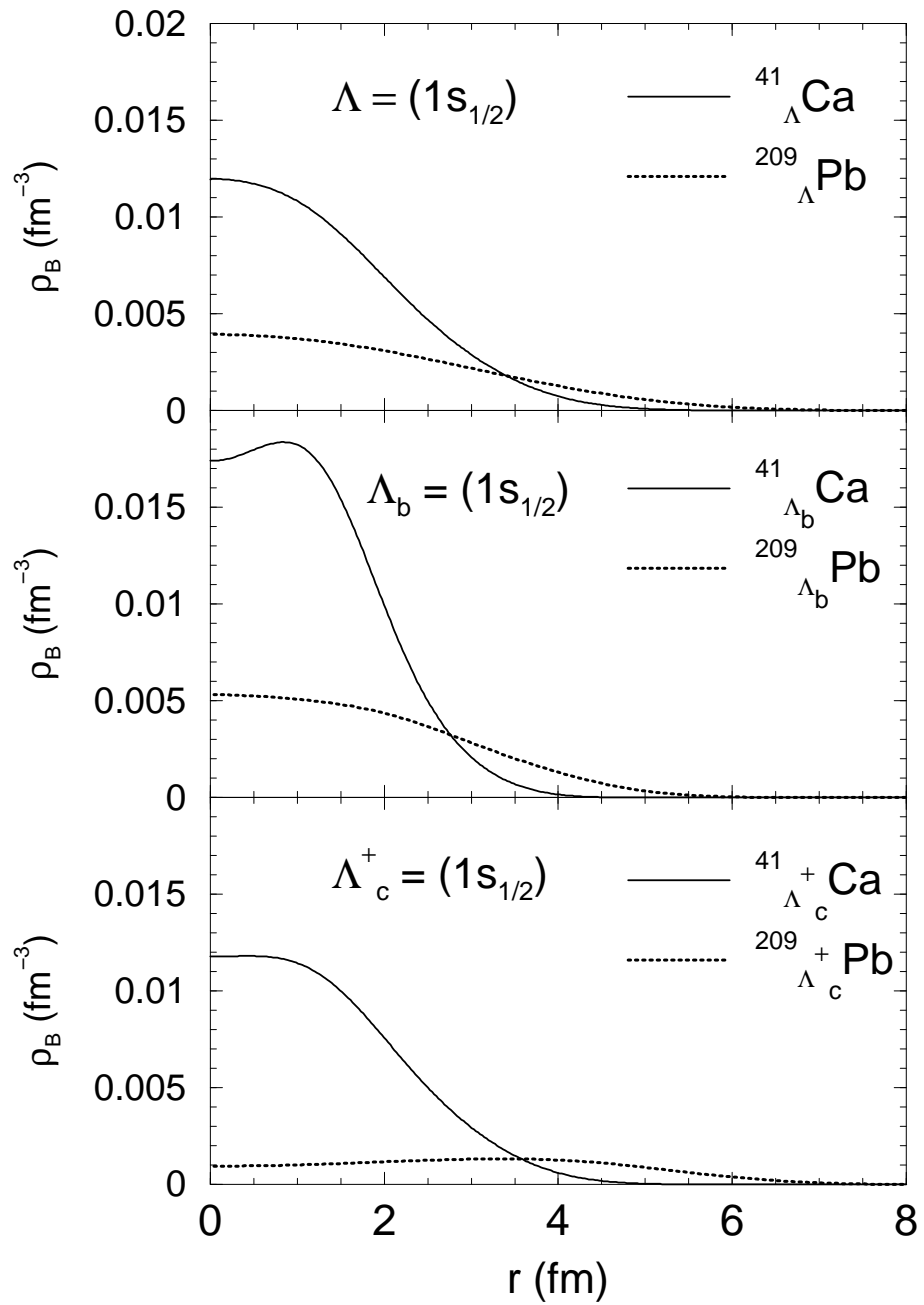


Figure 8: Λ , Λ_c^+ and Λ_b baryon (probability) density distributions for the $1s_{1/2}$ state in $^{41}_j\Lambda$ Ca and $^{209}_j\Lambda$ Pb ($j = \Lambda, \Lambda_c^+, \Lambda_b$).

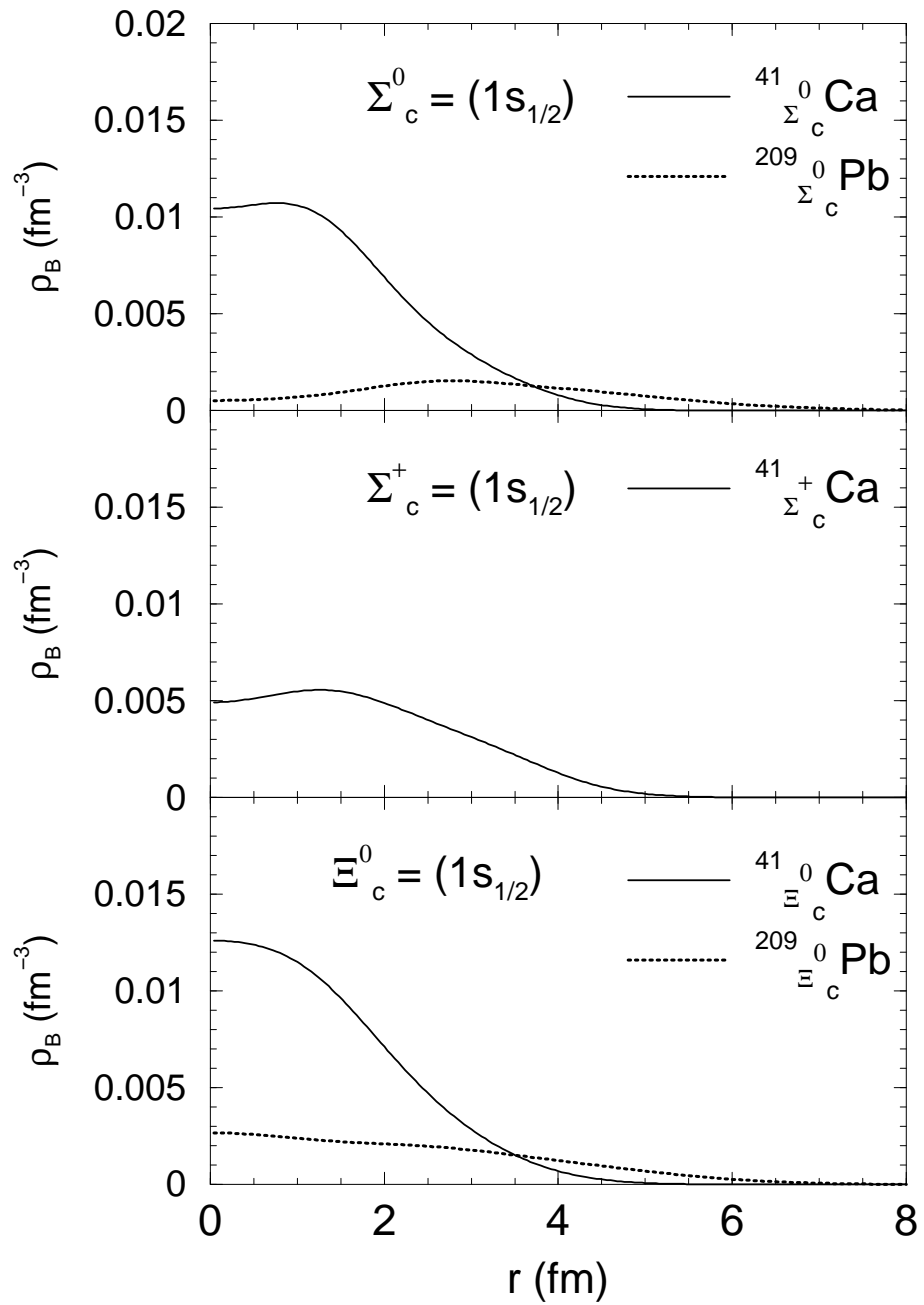


Figure 9: $\Sigma_c^{0,+}$ and Ξ_c^0 baryon (probability) density distributions for the $1s_{1/2}$ state in $^{41}_j\text{Ca}$ and $^{209}_j\text{Pb}$ ($j = \Sigma_c^{0,+}, \Xi_c^0$).